EPRI | ELECTRIC POWER RESEARCH INSTITUTE

Corrosion Effects and Prevention in Pipe-Type Cable Systems

Cathodic Disbondment Test Bed Development

1021887

Corrosion Effects and Prevention in Pipe-Type Cable Systems

Cathodic Disbondment Test Bed Development

1021887

Technical Update, December 2011

EPRI Project Manager

N. Murray

ELECTRIC POWER RESEARCH INSTITUTE
3420 Hillview Avenue, Palo Alto, California 94304-1338 ▪ PO Box 10412, Palo Alto, California 94303-0813 ▪ USA
800.313.3774 ▪ 650.855.2121 ▪ askepri@epri.com ▪ www.epri.com

DISCLAIMER OF WARRANTIES AND LIMITATION OF LIABILITIES

THIS DOCUMENT WAS PREPARED BY THE ORGANIZATION(S) NAMED BELOW AS AN ACCOUNT OF WORK SPONSORED OR COSPONSORED BY THE ELECTRIC POWER RESEARCH INSTITUTE, INC. (EPRI). NEITHER EPRI, ANY MEMBER OF EPRI, ANY COSPONSOR, THE ORGANIZATION(S) BELOW, NOR ANY PERSON ACTING ON BEHALF OF ANY OF THEM:

(A) MAKES ANY WARRANTY OR REPRESENTATION WHATSOEVER, EXPRESS OR IMPLIED, (I) WITH RESPECT TO THE USE OF ANY INFORMATION, APPARATUS, METHOD, PROCESS, OR SIMILAR ITEM DISCLOSED IN THIS DOCUMENT, INCLUDING MERCHANTABILITY AND FITNESS FOR A PARTICULAR PURPOSE, OR (II) THAT SUCH USE DOES NOT INFRINGE ON OR INTERFERE WITH PRIVATELY OWNED RIGHTS, INCLUDING ANY PARTY'S INTELLECTUAL PROPERTY, OR (III) THAT THIS DOCUMENT IS SUITABLE TO ANY PARTICULAR USER'S CIRCUMSTANCE; OR

(B) ASSUMES RESPONSIBILITY FOR ANY DAMAGES OR OTHER LIABILITY WHATSOEVER (INCLUDING ANY CONSEQUENTIAL DAMAGES, EVEN IF EPRI OR ANY EPRI REPRESENTATIVE HAS BEEN ADVISED OF THE POSSIBILITY OF SUCH DAMAGES) RESULTING FROM YOUR SELECTION OR USE OF THIS DOCUMENT OR ANY INFORMATION, APPARATUS, METHOD, PROCESS, OR SIMILAR ITEM DISCLOSED IN THIS DOCUMENT.

REFERENCE HEREIN TO ANY SPECIFIC COMMERCIAL PRODUCT, PROCESS, OR SERVICE BY ITS TRADE NAME, TRADEMARK, MANUFACTURER, OR OTHERWISE, DOES NOT NECESSARILY CONSTITUTE OR IMPLY ITS ENDORSEMENT, RECOMMENDATION, OR FAVORING BY EPRI.

THE FOLLOWING ORGANIZATION(S), UNDER CONTRACT TO EPRI, PREPARED THIS REPORT:

Electric Power Research Institute (EPRI)

This is an EPRI Technical Update report. A Technical Update report is intended as an informal report of continuing research, a meeting, or a topical study. It is not a final EPRI technical report.

NOTE

For further information about EPRI, call the EPRI Customer Assistance Center at 800.313.3774 or e-mail askepri@epri.com.

Electric Power Research Institute, EPRI, and TOGETHER…SHAPING THE FUTURE OF ELECTRICITY are registered service marks of the Electric Power Research Institute, Inc.

Copyright © 2011 Electric Power Research Institute, Inc. All rights reserved.

ACKNOWLEDGMENTS

The following organization prepared this report:

Electric Power Research Institute (EPRI)
1300 West W.T. Harris Blvd.
Charlotte, NC 28262

Principal Investigator
N. Murray

This report describes research sponsored by EPRI.

This publication is a corporate document that should be cited in the literature in the following manner:

Corrosion Effects and Prevention in Pipe-Type Cable Systems: Cathodic Disbondment Test Bed Development. EPRI, Palo Alto, CA: 2011. 1021887.

ABSTRACT

Coating disbondment, a common type of flaw in pipe-type transmission cables, can lead to serious corrosion problems. Flaws of known size and location are required to qualify new and emerging technologies or techniques as potential screening or predictive inspection tools for the management of coating disbondment. This report describes the development of a methodology based on novel methods of electrochemistry that can create locations of coating disbondment on the steel pipes used in pipe-type transmission cables.

Evaluation of screening and predictive technologies in a controlled environment determines their sensitivity, accuracy, and potential for finding flaws that have resulted from corrosion activity on a structure. Once the new technologies have been categorized as a predictive or screening tool, evaluations are made in an environment with greater variability. This stage is designed to study the effects of environmental factors such as temperature, humidity, solar radiation, and wind. The final stage of development is to migrate these technologies to the field where the operational aspects of the technology are studied, and additional factors can be added to the evaluation. These factors include circulating currents, additional types of corrosion, and stray currents from nearby agricultural or industrial activity. Samples with coating disbondment flaws of known size and location are required to undertake all of these stages of development.

Keywords
Cathodic disbondment
Electrochemistry
Corrosion
Pipe-type cable
Inspection
Asset management

CONTENTS

1 BACKGROUND 1-1

2 APPROACH 2-1

3 TEST SPECIMEN DEVELOPMENT 3-1

4 TEST BED DESIGN AND DEVELOPMENT 4-1

Test Bed Commissioning and Troubleshooting 4-4

Corrosion Test Cell Leakage Test 4-4

Heating Circuit Leakage Test 4-5

Heating Circuit Thermal Test: 4-5

Cathodic Disbondment Baseline 4-5

Electrochemical Impedance Spectroscopy (EIS) Baseline 4-6

5 CATHODIC DISBONDMENT TEST 5-1

Method Development 5-1

Approach 5-1

Equipment Requirements 5-2

Reagents and Materials 5-4

Cathodic Disbondment Procedure 5-6

Electrical Monitoring Schedule 5-6

Test Considerations 5-8

6 ELECTROCHEMICAL IMPEDANCE SPECTROSCOPY (EIS) 6-1

EIS Overview 6-1

Traditional Test Setup 6-2

Performance Criteria 6-3

Test Considerations 6-3

Graphical Interpretation of the Six Stages of Coating Degradation 6-3

7 PASSIVE HALF CELL ASSESSMENT 7-1

8 TEST DATA AND ANALYSIS RESULTS 8-1

Test Cell Visual Inspection 8-1

Cathodic Disbondment Data 8-5

Ultrasonic Thickness Testing 8-9

Electrochemical Impedance Spectroscopy (EIS) 8-13

9 CONCLUSIONS 9-1

Cathodic Disbondment Testing 9-1

Electrochemical Impedance Testing 9-1

Observations 9-1

Ultrasonic Testing 9-3

***10* FUTURE WORK 10-1**

***A* REFERENCES A-1**

***B* TEST BED COMMISSIONING PROTOCOL B-1**

Test Bed Commissioning and Data Collection Outline: B-1

***C* COATING ADHESION TEST C-1**

Adhesion Testing per ASTM D4541 - 02 ..... C-1

***D* REFERENCE CELL DATA CONVERSIONS D-1**

LIST OF FIGURES

Figure 1-1 Modeling a coating system using traditional electronic terminology 1-1
Figure 3-1 High voltage holiday testing the pipe sections 3-1
Figure 3-2 Installation of one test spool in the vault (L) and one installed in the cathodic disbondment test jig (R) 3-2
Figure 3-3 Test pipe spools that can be inserted in the underground test facility system 3-2
Figure 3-4 Three backfill types utilized in the underground test facilities 3-3
Figure 4-1 Heat cycle and pressure relief valve components 4-1
Figure 4-2 Ball valve for draining the oil from the test spool at the end of the testing 4-2
Figure 4-3 Lower half of the test cell (L) with a close up of the seal groove (R) 4-3
Figure 4-4 Upper half of the test cell (L) showing the two test ports with rubber bungs installed and all four ports in-service (R) 4-3
Figure 4-5 Cathodic disbondment test bed assembly (L) with check valves and PVC fittings installed 4-4
Figure 4-6 Thermal cycle programmed into to the controller 4-5
Figure 4-7 Counter to working electrode, laboratory noise due to unknown source (cabinet in dry cycle) 4-6
Figure 4-8 ac output from isolation transformer 4-7
Figure 4-9 Spectral analysis of isolation transformer output 4-7
Figure 4-10 ac output of Gamry transformer 4-8
Figure 4-11 Spectral analysis of Gamry transformer output 4-8
Figure 4-12 Counter to working electrode, laboratory noise due to unknown source (cabinet in humidity cycle) 4-9
Figure 4-13 Spectral analysis of laboratory noise (cabinet in humidity cycle) 4-9
Figure 4-14 Counter to working electrode, laboratory noise due to an unknown source 4-10
Figure 4-15 Spectral analysis of laboratory noise (with scope inside of faraday cage) 4-10
Figure 4-16 Earth ground to faraday cage with the potentiostat chassis grounded 4-11
Figure 4-17 Spectral analysis of the earth ground to faraday cage 4-11
Figure 4-18 Earth to faraday cage without the potentiostat ground 4-12
Figure 4-19 Spectral analysis of earth ground to faraday cage with potentiostat ground removed 4-12
Figure 5-1 Cathodic disbondment test set-up per modified ASTM G42 5-5
Figure 5-2 Coating disbondment test jig for development of hidden corrosion cells 5-6
Figure 5-3 Illustrates the power supply, thermal controller and heater chiller 5-7
Figure 6-1 Test set-up for EIS testing 6-2
Figure 8-1 Disassembling the test cell for inspection was complicated due to the harsh test environment 8-1
Figure 8-2 The test cell had indications of corrosion within the bolt pattern 8-2
Figure 8-3 Lower housing of the test cell showing corrosion 8-3
Figure 8-4 Upper test cell housing 8-4
Figure 8-5 Illustrates the corrosion originating at the test ports 8-4
Figure 8-6 Cathodic disbondment data at ambient temperatures 8-7
Figure 8-7 Cathodic disbondment data at elevated temperatures 8-8
Figure 8-8 Ambient temperature changes within the corrosion laboratory 8-9
Figure 8-9 Mapping the thickness of the coating and pipe wall 8-10
Figure 8-10 Mapping the disbondment area using a 1 in. x 1 1/4 in. grid 8-11
Figure 8-11 Graphical representation illustrating the ultrasonic thickness data 8-13
Figure 8-12 Open circuit potential (OCP) of the test spool before conducting the EIS test 8-14
Figure 8-13 Levenberg-Marquardt Method using a traditional paint model 8-15

Figure 8-14 Levenberg-Marquardt Method using a rapid assessment model.....8-16
Figure 8-15 Simplex method using a traditional paint model 8-16
Figure 8-16 Simplex method using a traditional rapid assessment model.....8-17
Figure 9-1 Graphical representation of EIS results.....9-2

LIST OF TABLES

Table 4-1 Characteristics of oil candidates to be used for heating the test spool 4-2
Table 4-2 Harmonic frequencies and sources found during testing 4-13
Table 6-1 Example of EIS measurements before and after hot acidic immersion exposure testing 6-2
Table 8-1 Cathodic disbondment data during the elevated temperatures 8-5
Table 8-2 Cathodic disbondment data during the ambient temperatures 8-6
Table 8-3 Utrasonic thickness inspection data 8-12
Table 8-4 Water sample resistances 8-14
Table 8-5 Summary results for the four analysis methods utilized 8-17
Table 9-1 Electrochemical impedance spectroscopy results 9-2
Table C-1 Examples of disbondment due to tensile testing C-1
Table D-1 Conversion chart for different types of reference electrodes D-1

1
BACKGROUND

Disbonded coating systems on direct buried pipe have been identified as the most problematic maintenance issue faced by asset managers of pipe-type underground transmission systems. This is due to the fact that the coating systems are highly efficient dielectric barriers and engineered backfills attenuate guided waves that are injected into the pipe wall. The combination of the two properties prevents the use of traditional pipeline inspection techniques.

The following are the events leading to the degradation of a pipe type cable installation.

- Intact Coating Systems shield the Pipe from Cathodic Protection
- Coating Permeability Increases due to Thermal Load & Moisture Adsorption
- Moisture Tunnels Through Pores in Coating System to Base Metal Substrate
- Moisture in Pit Becomes Highly Acidic
- Accelerated Corrosion Cell Established Below Coating
- Coating Disbonds and Corrosion Products Expand Under Coating

Coating systems can be modeled (Figure 1-1) by designing circuitry that mirrors components of a corrosion cell. Coating and corrosion (byproducts) films have measureable capacitance values and the coating system containing solution filled pores have measureable resistance. Each of these components change as the system degrades and can be quantified by electrochemical test methods.

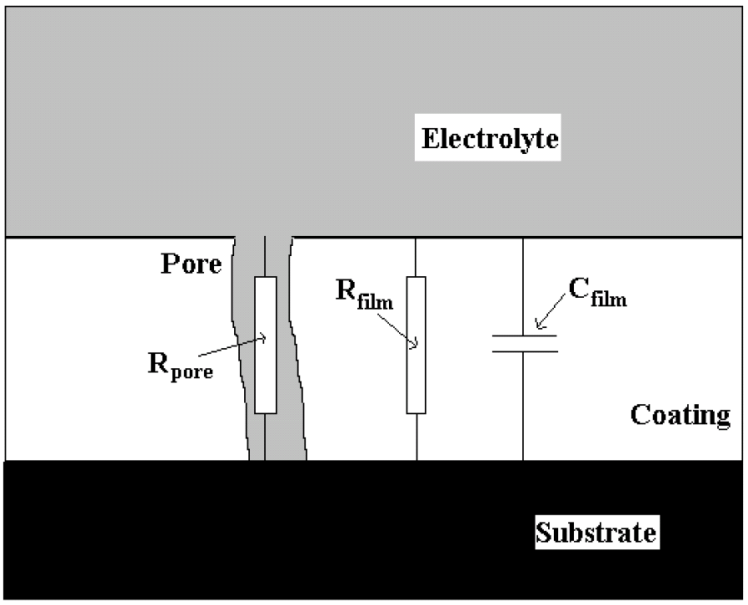


Figure 1-1
Modeling a coating system using traditional electronic terminology

Coating systems all have some degree of permeability and over time will allow moisture to penetrate, disbond the edges of the pores and then pond under the disbonded area. This stagnant water will form a corrosion cell that accumulates an increasing concentration of ionic species with the associated decrease in pH levels. This change in pH [-log10(aH+)] is a measure of anion and cation content of a solution and directly influences the severity of the corrosion cell as the acidity level increases. There are many types of corrosion that can occur on a pipe with an open, disbonded coating; however localized corrosion or pitting corrosion is dominant in sealed, disbonded coating areas. In sustained localized corrosion the penetration rate is of concern because the pipe contains pressurized fluids and will rupture when the hoop stresses exceed the tensile strength of the material.

The dielectric fluid used within the pipes is a mineral oil and should breakdown in the soils through natural metabolic activity when there is a leak. Decomposition of the oil droplets are a function of both surface area and the lack of nutrients such as nitrogen and phosphorus. If these conditions are not met then the release of fluids should be considered detrimental to the environment and a hazardous spill requiring soil remediation. Mineral oil adsorbs very well on smectite (bentonite) clays, or on peat moss, which may retain the spill for some period of time. If the leakage rate is extreme then the cooling ability of the system may be compromised and a thermal excursion could occur resulting in outages or brownouts.

Gaps have been identified in areas of inspection, assessment and mitigation of pipe type cable systems. Research completed in 2010 (EPRI Report PID 1011110) demonstrated that guided wave technologies have limitations due to attenuation of the signals and sectional losses could not reliably be identified at distances greater than 10 feet. Electrochemical technologies borrowed from pipeline inspections are also limited by the dielectric properties of the coating systems when there is a disbondment without a breach or holiday.

2
APPROACH

The focus of this project is to develop a methodology for flaw insertion which results in a coating system disbondment without a holiday. Once this methodology is perfected on test spools in the laboratory the flaws are assessed using state of the art inspection technologies.

If these technologies are proven to have merit as an inspection technology the evaluations will then be expanded to the underground test facilities where additional environmental factors are added to the inspections. This is a critical phase to complete before any field inspections are completed at customer service areas.

The goal at this point is to assess the technologies and determine if they are best suited as a screening tool or predictive technology. The field assessments following this phase will then quantify the technology in terms of accuracy, risk, cost and probability of locating disbonded coating systems.

3
TEST SPECIMEN DEVELOPMENT

To support the test facility evaluations mechanical flaws were inserted in long pipe sections in various backfill materials to provide an environment for additional assessments and development. This supports the traditional pipeline test techniques where there is coating disbondment and the resulting sectional loss. The test facility piping has impressed current cathodic protection systems installed and maintains the installed sectional loss levels and associated coating disbondment.

The center vault contains a spool piece with 300# flanges welded onto both ends and the coating system was holiday tested per ASTM D5162 - 08 Method B [11]. Figure 3-1 illustrates the use of a high voltage holiday tester to confirm that there are no coating imperfections or discontinuities in the test pipes.



Figure 3-1
High voltage holiday testing the pipe sections

Two spool pieces were fabricated with the installation of the first one in the underground test facility center vault. The second spool piece was reserved for installation into a cathodic disbondment test jig in the corrosion laboratory. Figure 3-2 illustrates the two test spools installed for evaluation.



Figure 3-2
Installation of one test spool in the vault (L) and one installed in the cathodic disbondment test jig (R)

Both test spools were magnetic particle inspected for weld inclusions and then holiday tested and recoated where the welding process had damaged the coating system. Figure 3-3 illustrates the test spools and the coating repairs required due to fabrication damage.



Figure 3-3
Test pipe spools that can be inserted in the underground test facility system

Once the disbonded coating development method has been evaluated in the laboratory and within the vault, the flaws will be inserted into pipe sections that have been direct buried in various backfills. Figure 3-4 illustrates the three backfill types installed in the underground test facility. The first section has the native soil, the middle section has gravel with one foot of native soil and the last (nearest) has a sand/mortar mix backfill.



Figure 3-4
Three backfill types utilized in the underground test facilities

Once the method for insertion of disbonded coatings is perfected guided wave technologies can be evaluated in each backfill condition to understand attenuation properties and power requirements.

4
TEST BED DESIGN AND DEVELOPMENT

The concept of the test bed is to evaluate the coating system changes under real exposure conditions consisting of a large thermal gradient, induced direct currents and immersion service. To satisfy these parameters it was necessary to have multiple chambers in the test bed to allow a heating cycle representative of the conductor temperature at load and a test cell with an electrolyte kept at a constant 7.2°C (45°F).

The test specimen is described in the previous section; however the blind flanges were modified to accept a host of instrumentation and control loops. The one end contains the immersion heater, thermocouple and pressure relief valve. The immersion heater maintains a constant 93°C using a thermal controller with feedback from a thermocouple while the pressure relief valve dumps excess pressure that is generated by the thermal expansion of the heating oil.

Figure 4-1 shows the control end of the test spool with the heater element, thermocouple, safety relief valve, pressure gauge and the controller mounted on the test spool frame.

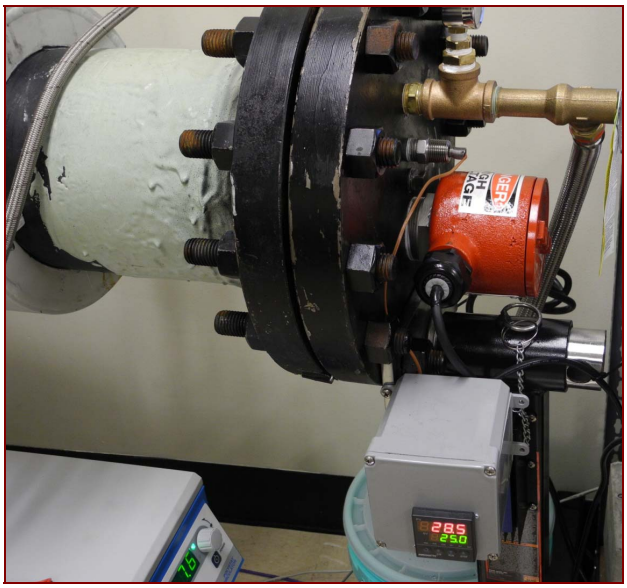


Figure 4-1
Heat cycle and pressure relief valve components

The other end of the test spool was modified by adding a ball valve for draining the oil at the completion on the testing and a fill vent to reduce trapped air at the top of the test spool pipe. Figure 4-2 shows the ball valve used to drain the oil from the test spool at the end of the testing.

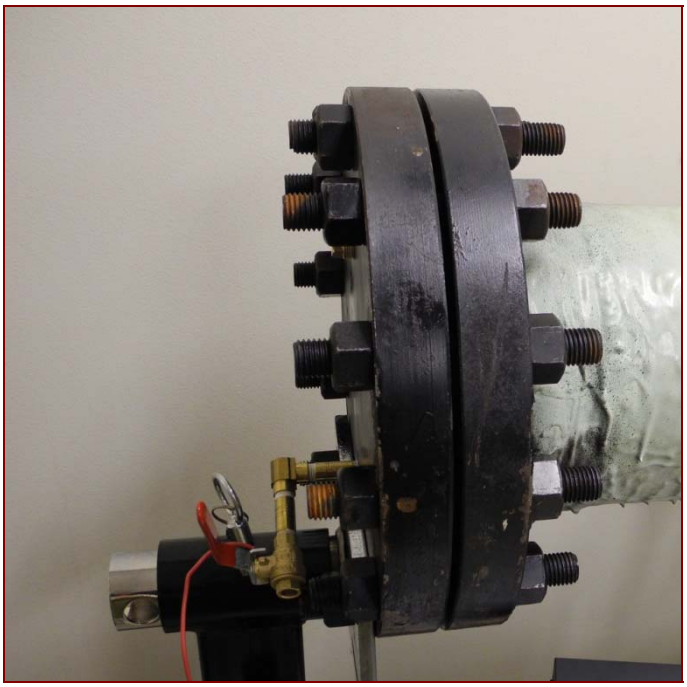


Figure 4-2
Ball valve for draining the oil from the test spool at the end of the testing

Transformer oil was initially identified for the heating cycle however canola oil (see Table 4-1) was identified as a better substitute due to environmental restrictions and a higher smoke point. Nine (9) gallons were purchased to fill the test spool.

Table 4-1
Characteristics of oil candidates to be used for heating the test spool

Characteristics	Canola Oil	Mineral Oil	Vegetable Oil
Color	Yellow	Clear	Yellow
Odor	Mild	Odorless	Mild
Physical State	Liquid	Liquid	Liquid
pH	6.6	Not Applicable	7
Smoke Point	204°C (400°F)	138°C (280°F)	182°C (360°F)
Flash Point	>260°C (500°F) (Cleveland Open Cup)	168.33°C (335°F) (Closed Cup)	327°C (620°F) (Cleveland Open Cup)
Vapor Pressure	< 0.05 mmHg @ 300°C	<0.1 kPa @ 20°C	0.7 psi @ 20°C
Specific Gravity	0.91–0.92 (25°C)	0.835 (15.6°C)	0.91–0.92 (25°C)

The test cell was fabricated as an annulus that clamps around the test spool. The test cell perimeter has a seal groove that has about 15% squeeze (compression) to contain the electrolyte which was used for both the cooling cycle and the EIS testing. The lower half of the test cell has a port installed for the cooling water outlet. Figure 4-3 shows the lower half of the test cell with alignment pins (left), after the assembly was powder coated. The seal groove and alignment pins (right) were masked to keep the surfaces flat and allow a good seal.

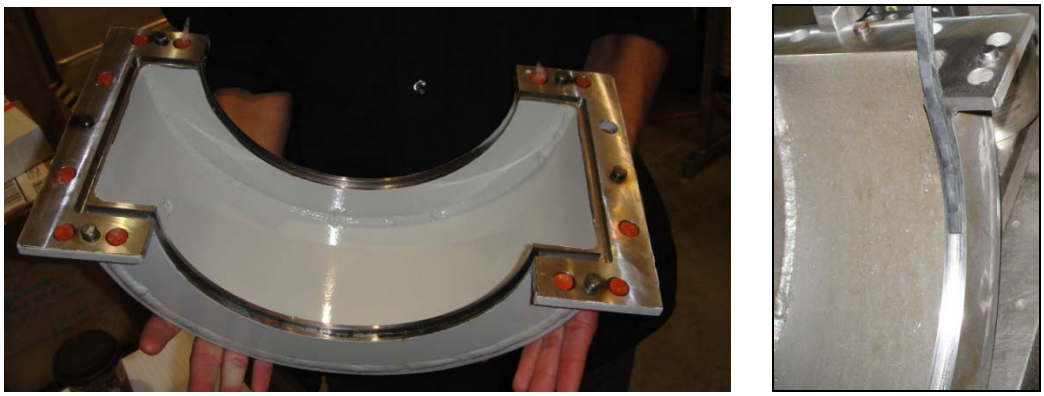


Figure 4-3
Lower half of the test cell (L) with a close up of the seal groove (R)

The upper half of the test cell has three ports installed, one for the inlet from the heater/ chiller and two for instrumentation. Figure 4-4 illustrates the two ports used for circulating the cooling water and the two ports used to monitor the cathodic disbondment.



Figure 4-4
Upper half of the test cell (L) showing the two test ports with rubber bungs installed and all four ports in-service (R)

A heater chiller was purchased to circulate the cooling water through the annulus. The connections to the test spool were made with stainless steel braided lines and the chiller was filled with distilled water from the distillation still. The test bed was assembled with quick disconnects with check valves for ease of repairs but also PVC fittings to isolate the heater/chiller ground from the test bed (see Figure 4-5).

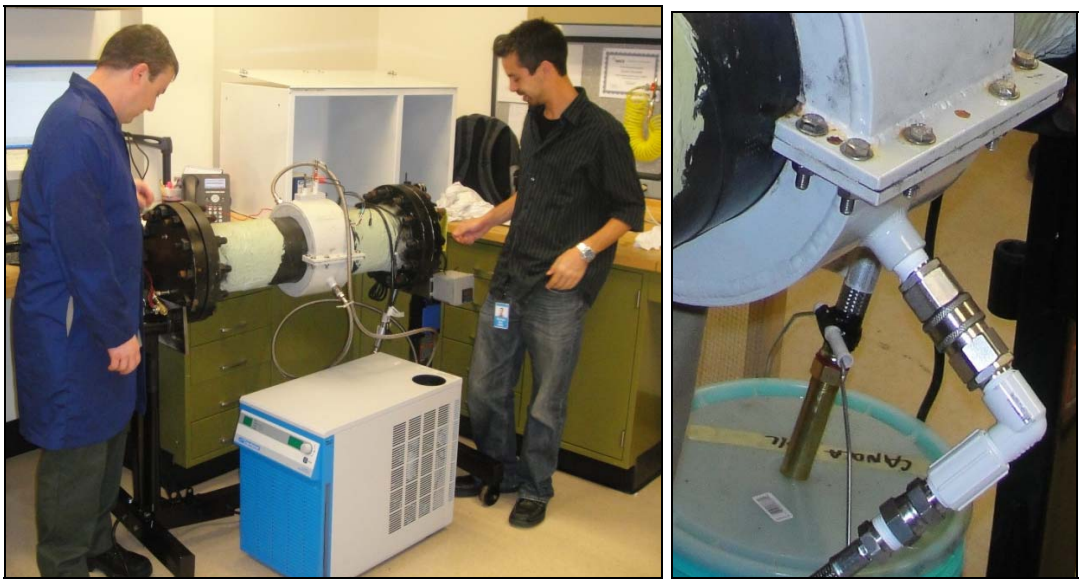


Figure 4-5
Cathodic disbondment test bed assembly (L) with check valves and PVC fittings installed

Test Bed Commissioning and Troubleshooting

Once the test bed was assembled each subsystem was tested and errors eliminated (see appendix B for the commissioning protocol). During the test bed commissioning and exposure testing there were many anomalies uncovered specific to this equipment configuration. The anomalies included coating capacitance, electrolyte resistance, thermal expansion, electrolyte leaks, oil leaks, emf and circulating currents. The greatest challenge was to eliminate the circulating ground currents, keeping the test cell isolated and not having floating grounds. PVC fittings (see Figure 4-5 right image) were added to the assembly to electrically isolate the grounding system of the heater chiller from the test spool. The evaluation of each subsystem was required and it was completed in the following sequence:

Corrosion Test Cell Leakage Test

The test cell initially leaked cooling water and it was determined that the seals compression of 7% was insufficient and it was increased to 15% by migrating to a seal with larger cross sectional area. A larger rectangular seal was purchased with grease impregnated in the fibers and RTV was added to the edge of the sealing channel. The test cell was reassembled and successfully pressurized to 10 psi without leakage.

Heating Circuit Leakage Test

Nine (9) gallons of canola oil were added to the test spool and it was noted that the heating circuit leaked from the heating element mounting threads. The heating element was removed, additional Teflon tape was added and the assembly tightened to the recommended torque setting (211 ft-lbs). This corrected the leakage from the heating element mounting threads.

Heating Circuit Thermal Test

The thermal cycle was tested for hysteresis and it was discovered that there would be a thermal excursion by 3°C to 5°C. The set point was changed to 93°C and the duration was set for 600 minutes before shutdown and the cool down period. Figure 4-6 illustrates the program for the thermal cycle where the system would shut down in the morning so that EIS testing could be completed.

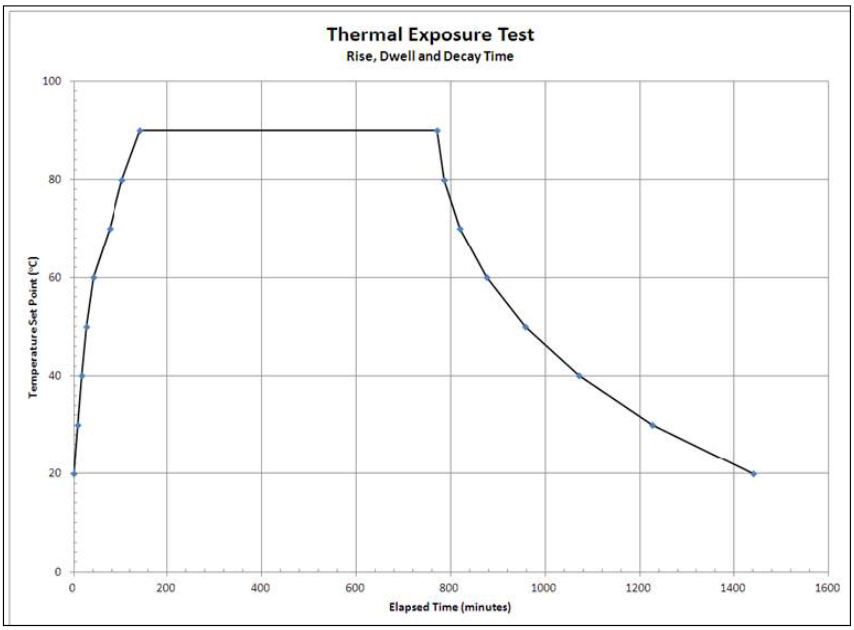


Figure 4-6
Thermal cycle programmed into to the controller

The test spool was heated to 50°C and the pressure due to thermal expansion noted as 90 psi. The lift lever on the safety relief valve was cycled and the pressure was reduced to a near constant 40 psi throughout the subsequent heat cycles.

Cathodic Disbondment Baseline

The cathodic disbondment exposure test uses a direct current from a power supply to cause the coating system to disbond. This was the only part of the exposure testing requiring a reference cell to monitor the polarization levels so it was decided to use a copper copper sulfate ($CuCuSO_4$) reference cell.

Electrochemical Impedance Spectroscopy (EIS) Baseline

There were many issues associated with measuring an EIS baseline on the test spool. The coating had zero defects and could be considered near perfect causing the potentiostat to operate at the high end of its performance limits. Most of the impedance values that were of interest were conducted at a frequency of 100 Hz and exceeded 950 MΩ. At these limits the test spool acted as an antenna picking up frequencies from many sources such as the florescent light ballast, the scanning electron microscope (SEM) in the next laboratory, the screw compressor in the shipping department and movement of personnel next to the test bed. A faraday cage was constructed that encased the entire test bed which removed the effects of most sources but further investigation was required.

Troubleshooting

An oscilloscope was connected between the graphite counter and working electrode (see Figure 4-4 (R)) to understand the source of the noise (see Table 4-2). Note that the orange electrode is the $CuCuSO_4$ reference electrode, the black electrode is the graphite counter electrode and the working electrode is the test spool. The scope trace (Figure 4-7) confirmed that there was a source for the noise.

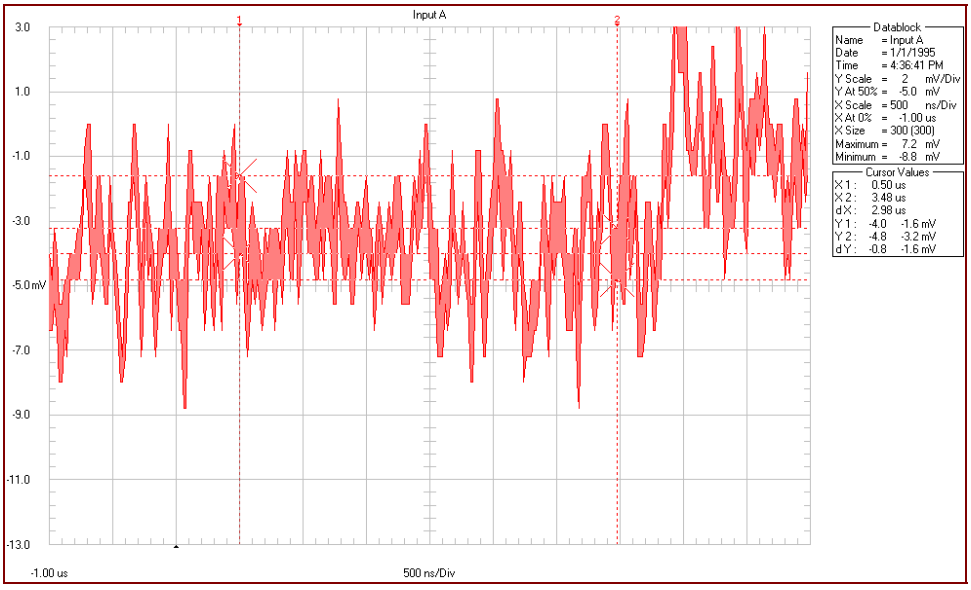


Figure 4-7
Counter to working electrode, laboratory noise due to unknown source (cabinet in dry cycle)

The scope was then connected to the isolation transformer to see if the signal was clean (Figure 4-8) and a fast fourier transform (FFT) was performed to measure the frequencies (Figure 4-9).

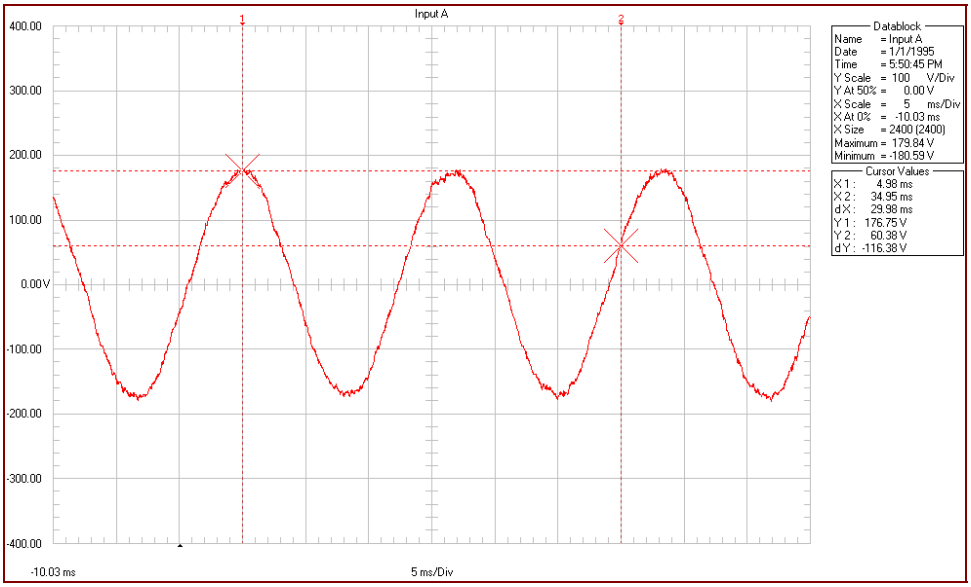


Figure 4-8
ac output from isolation transformer

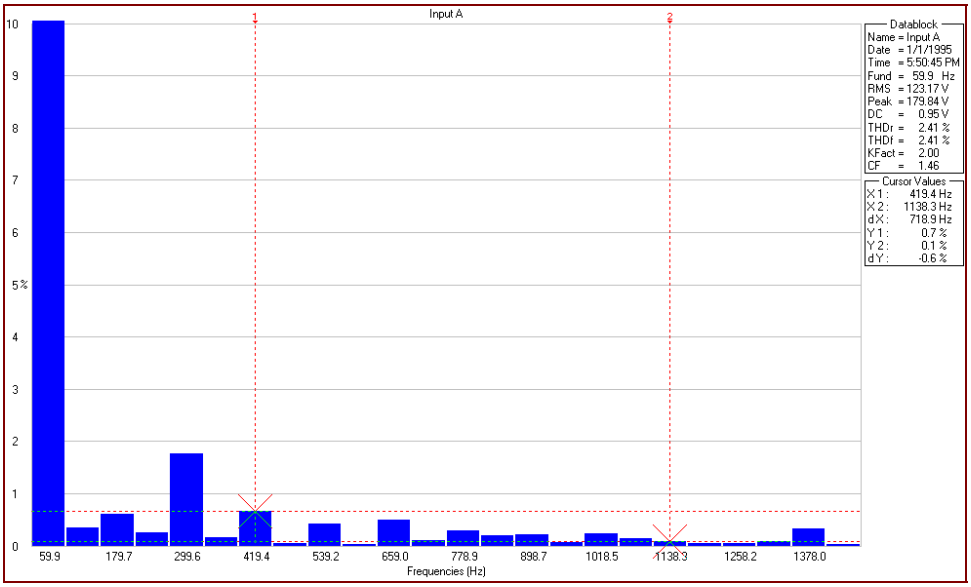


Figure 4-9
Spectral analysis of isolation transformer output

It was found that there were harmonic frequencies present, however the most significant frequency was at 300 hz and not considered an issue. The scope was then connected to the Gamry transformer to understand any noise present (see Figure 4-10) and then an FFT was performed to analyze the spectrum for harmonic frequencies (see Figure 4-11).

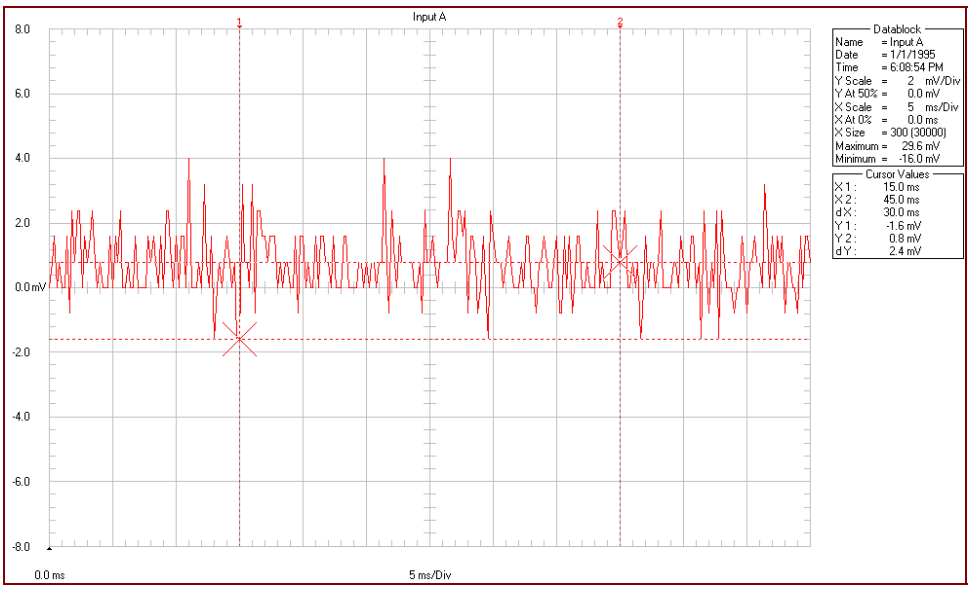


Figure 4-10
ac output of Gamry transformer

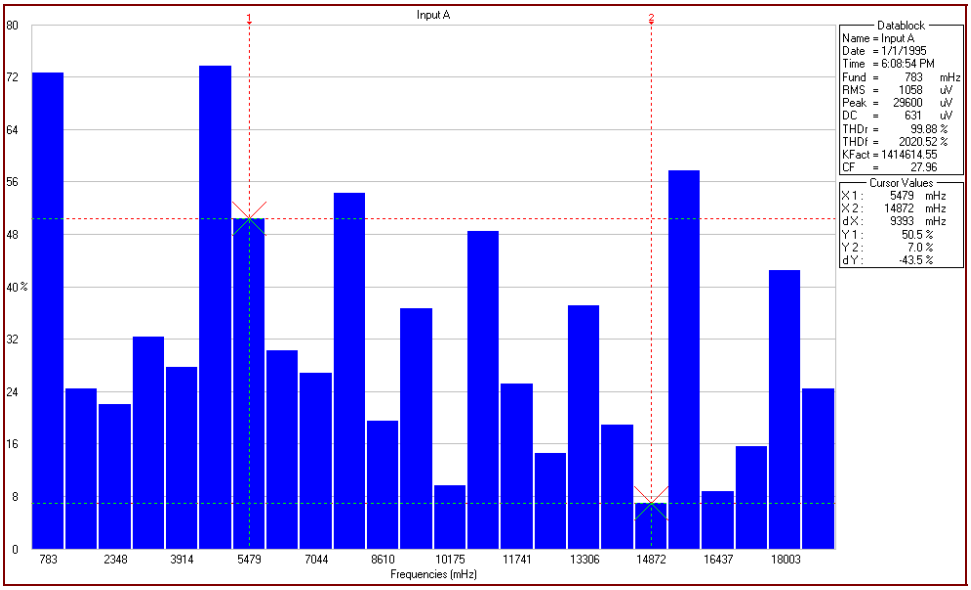


Figure 4-11
Spectral analysis of Gamry transformer output

The scope was reconnected to the counter and working electrode to again measure the noise. The lights were turned off and the cyclical exposure cabinet was changed to the humidity cycle (see Figure 4-12). The trace was then analyzed for harmonic frequencies (see Figure 4-13).

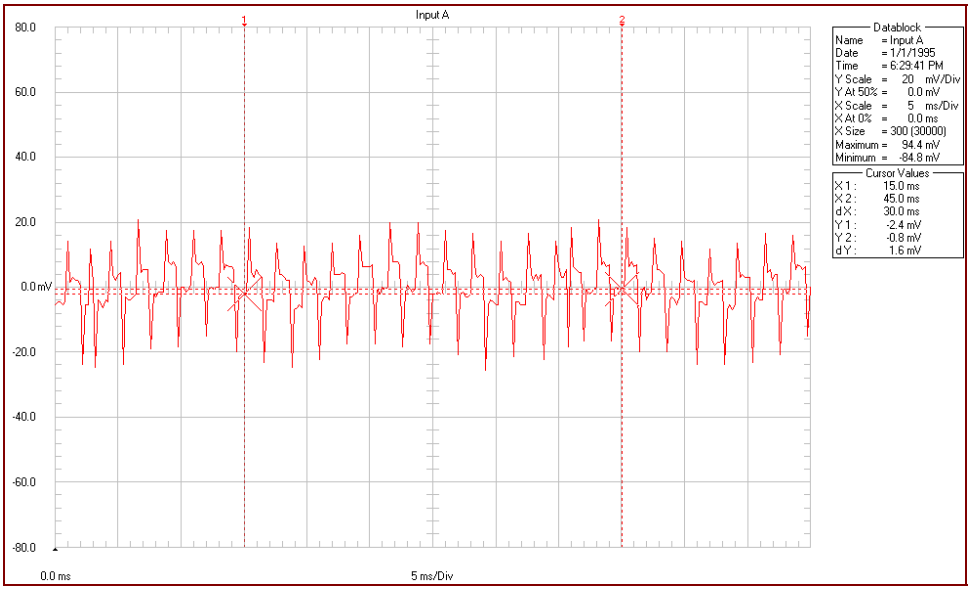


Figure 4-12
Counter to working electrode, laboratory noise due to unknown source (cabinet in humidity cycle)

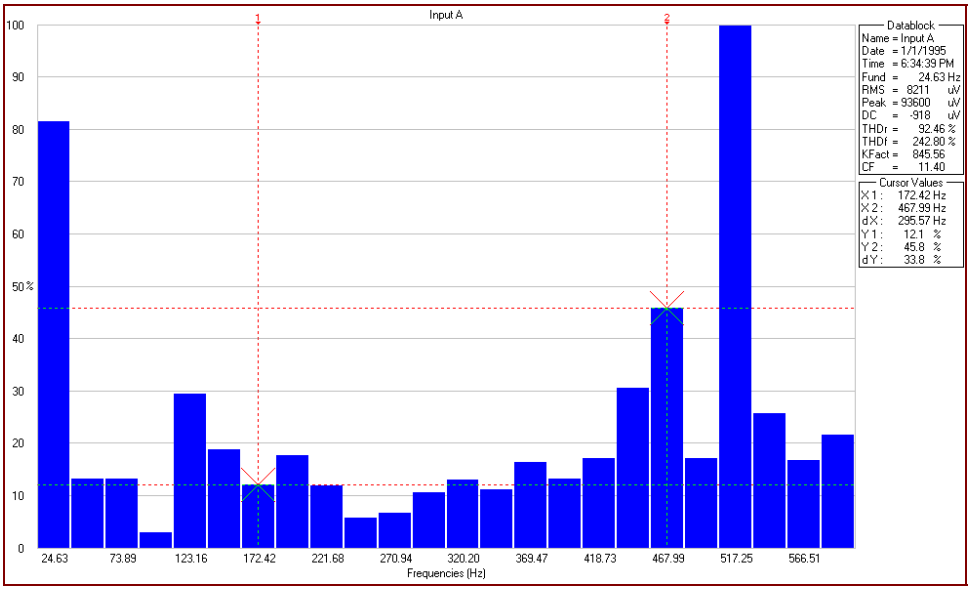


Figure 4-13
Spectral analysis of laboratory noise (cabinet in humidity cycle)

The frequency that dominated the spectral analysis was a harmonic and the source has still not been identified but it is suspected that it has to do with the exposure cabinet boiler system with that uses a blower to vacate the cabinet. The scope was relocated to the inside of the faraday cage and a trace captured (Figure 4-14). Neither frequency present in the FFT analysis (see Figure 4-15) seems to be a harmonic of the power supply frequency, however what was of interest was that 914Hz was not present in the previous trace that was captured outside the faraday cage.

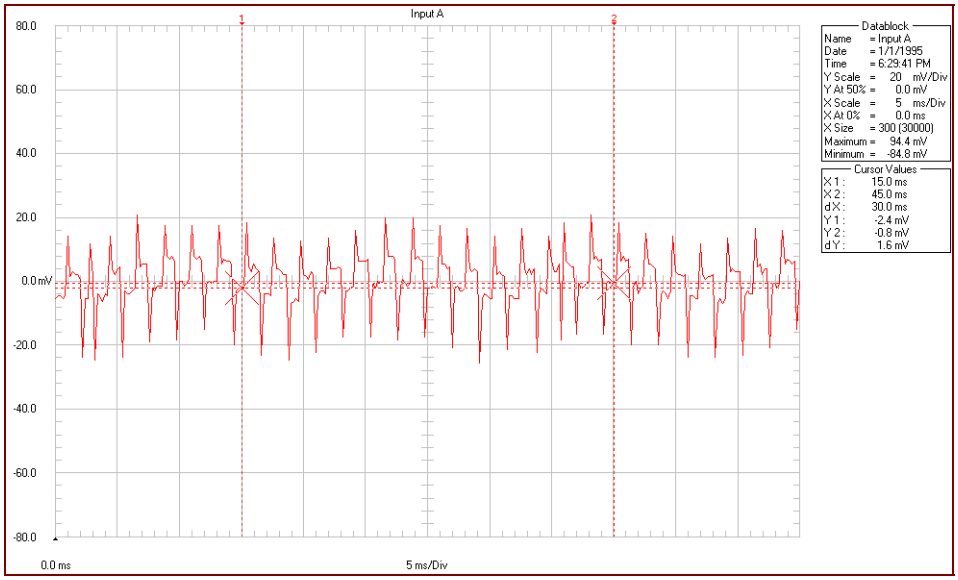


Figure 4-14
Counter to working electrode, laboratory noise due to an unknown source (Scope inside of faraday cage and cabinet in humidity cycle.)

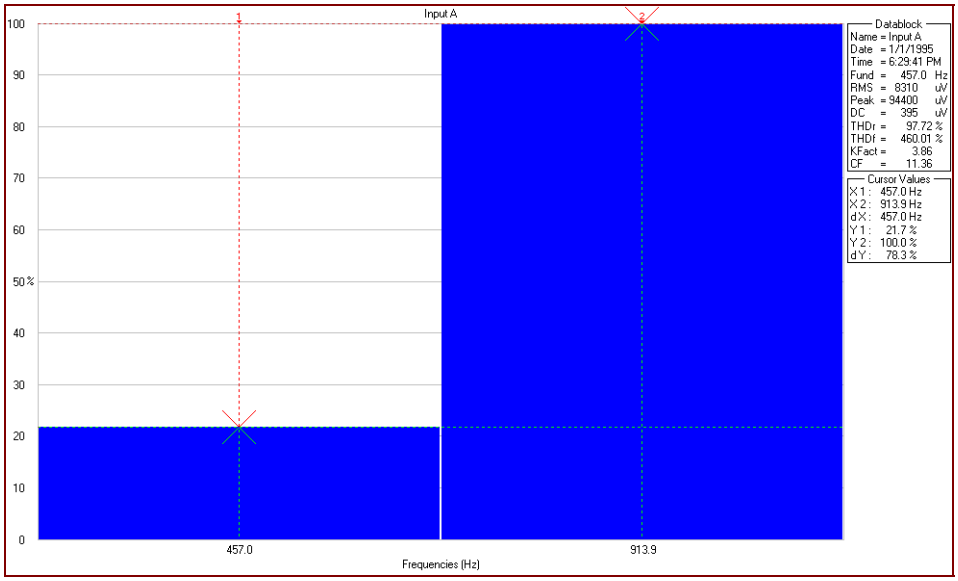


Figure 4-15
Spectral analysis of laboratory noise (with scope inside of faraday cage)

The scope was then attached between the earth ground and the faraday cage to see if there were any circulating currents through the potentiostat chassis (see Figure 4-16) and a 400 mV signal was detected.

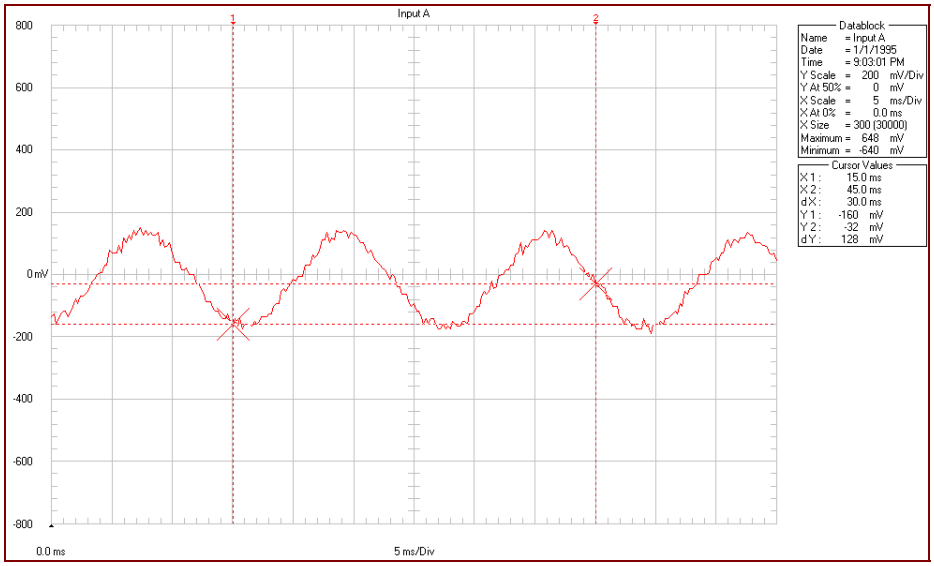


Figure 4-16
Earth ground to faraday cage with the potentiostat chassis grounded

The scale of the FFT was changed to 10% and it was determined that all of the frequencies were a harmonic of the Ac power supply (Figure 4-17).

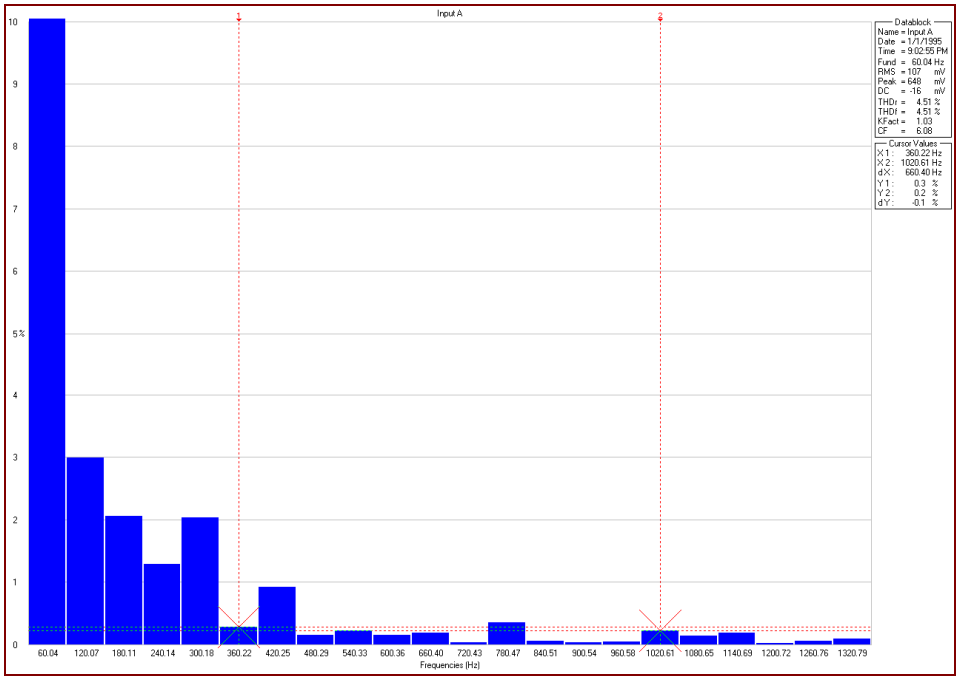


Figure 4-17
Spectral analysis of the earth ground to faraday cage

The potentiostat was disconnected and the earth ground to the faraday cage was again reviewed (Figure 4-18) for noise. A spectral analysis (Figure 4-19) was then completed and the second harmonic increased while all the remaining ones decreased.

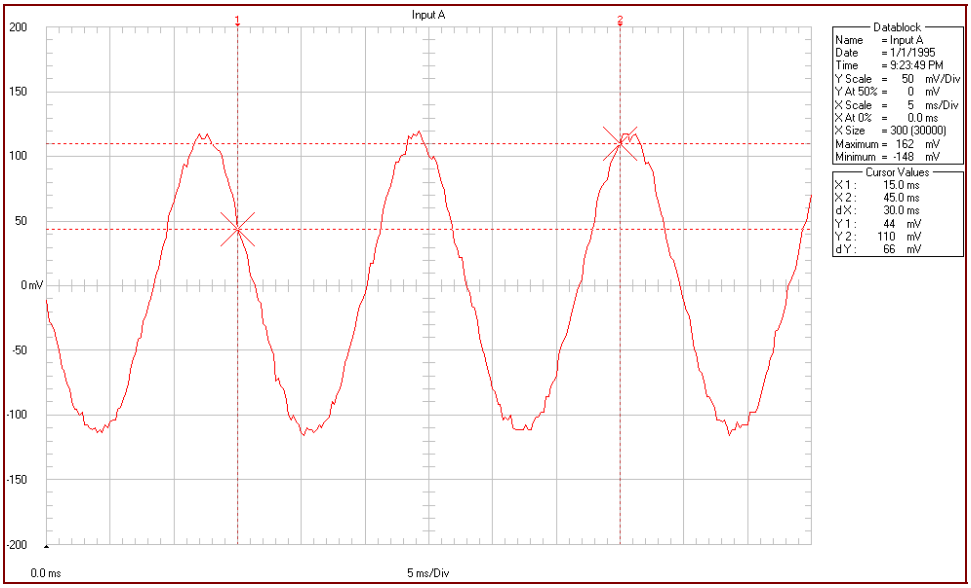


Figure 4-18
Earth to faraday cage without the potentiostat ground

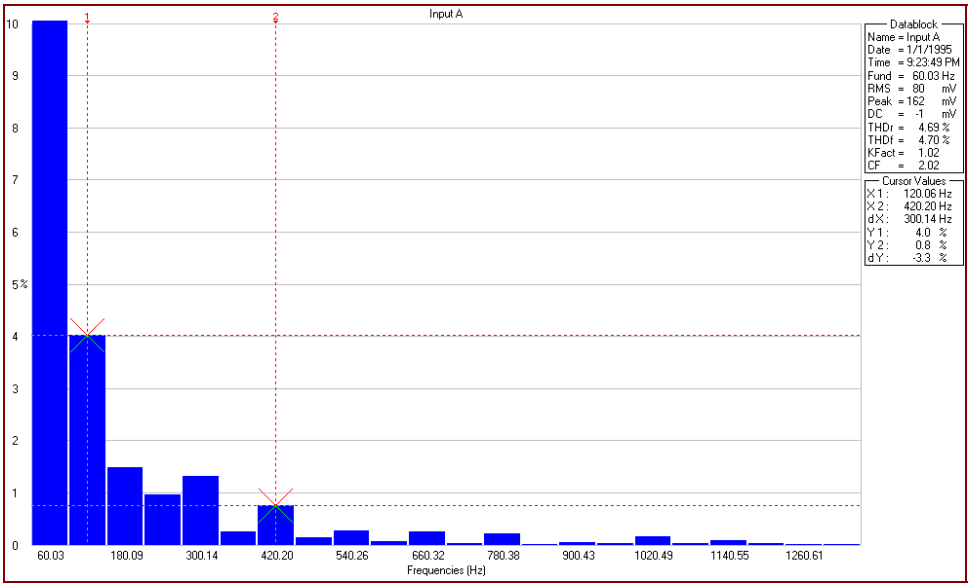


Figure 4-19
Spectral analysis of earth ground to faraday cage with potentiostat ground removed

Keeping the potentiostat chassis grounded to the faraday cage reduced the voltage of the secondary haramonic but increased the first and third harmonic voltages.

Table 4-2
Harmonic frequencies and sources found during testing

Measurement Points	Frequency	Unit	Voltage	Unit	Frequency	Unit	Voltage	Unit	Frequency	Unit	Voltage	Unit	Notes
Output from Isolation Transformer	59.9	Hz	174.1	V	299.6	Hz	3.1	V	419.4	Hz	1.2	V	
Counter to Working	517.3	Hz	172.0	μV	24.6	Hz	140.0	μV	468.0	Hz	79.0	μV	Faraday cage, Dry cycle
Gamry Power Supply	783.0	mHz	30.0	μV	4,696.0	mHz	30.0	μV	15,654.0	mHz	24.0	μV	
Counter to Working	517.3	Hz	172.0	μV	492.6	Hz	140.0	μV	468.0	Hz	79.0	μV	Faraday cage, Humidity cycle
Counter to Working	913.9	Hz	37.0	μV	457.0	Hz	47.0	μV					Faraday cage, Humidity cycle, Scope in faraday cage
Earth to Faraday Cage	60.0	Hz	148.0	mV	120.1	Hz	4.0	mV	180.1	Hz	3.0	mV	Faraday cage, Humidity cycle, Scope in faraday cage
Earth to Faraday Cage	60.0	Hz	113.0	mV	120.1	Hz	5.0	mV	180.1	Hz	2.0	mV	Faraday cage, Humidity cycle, Scope in faraday cage, Potentiostat Disconnected

Elevated Test Temperatures

Initially the hope was to conduct the impedance testing at elevated temperatures which would provide corrosion rates that were representative of the pipe while in-service. It was determined that most reference cells could not operate at elevated temperatures for sustained periods of time. The hydrogen reference cell had too large an impedance value to allow a three electrode test so the configuration was changed to a two electrode system and all EIS tests were conducted at ambient (room) temperatures.

5
CATHODIC DISBONDMENT TEST

To evaluate and compare the affect of cathodic reaction products at pinholes or mechanically damaged areas and how well a coating adheres to the substrate in case there is discontinuity. These holidays are not detectable through typical passive half cell techniques but only through the pore development detectable through EIS and trended through changes in capacitance, moisture absorption and pore resistance. ASTM G42 is modified to eliminate the insertion of a holiday, requiring the use of EIS and current density measurements to trend the change.

Method Development

1. This test method covers accelerated procedures for simultaneously determining comparative characteristics of coating systems applied to steep pipe exterior for the purpose of preventing or mitigating corrosion that may occur in underground service where the pipe will be in contact with natural soils and will receive cathodic protection. They are intended for use with samples of coated pipe taken from commercial production and are applicable to such samples when the coating is characterized by function as an electrical barrier.
2. This test method is intended to facilitate testing of coatings where the test cell is cemented to or clamped to the surface of the coated pipe specimen. This is appropriate when it is impractical to submerge or immerse the test specimen as required by Test Methods ASTM G 8, G 42, or G 80[3,5]. Coating sample configuration such as flat plate and small diameter pipe may be used, provided that the test procedure remains unchanged. This test method allows options that must be identified in the report.

Approach

1. Damage to pipe coating is almost unavoidable during transportation and construction. Breaks or holidays in pipe coatings may expose the pipe to possible corrosion since, after a pipe has been installed underground, the surrounding earth will be moisture-bearing and will constitute an effective electrolyte. Applied cathodic protection potentials may cause loosening of the coating, beginning at holiday edges. Spontaneous holidays may also be caused by such potentials. This test method provides accelerated conditions for cathodic disbondment to occur and provides a measure of resistance of coatings to this type of action.
2. The effects of the test are to be evaluated by physical examinations and monitoring the current drawn by the test specimen. Usually there is no correlation between the two methods of evaluation, but both methods are significant. Physical examination consists of assessing the effective contact of the coating with the metal surface in terms of observed differences in the relative adhesive bond. It is usually found that the cathodically disbonded area propagates from an area where adhesion is zero to an area where adhesion reaches the original level. An intermediate zone of decreased adhesion may also be present.

3. Assumptions associated with test results include:

   a. Maximum adhesion, or bond, is found in the coating that was not immersed in the test liquid.

   b. Decreased adhesion in the immersed test area is the result of cathodic disbondment.

   c. Ability to resist disbondment is a desired quality on a comparative basis, but disbondment in this test method is not necessarily an adverse indication of coating performance. The virtue of this test method is that all dielectric-type coatings now in common use will disbond to some degree, thus providing a means of comparing one coating to another.

   d. The current density appearing in this test method is much greater than that usually required for cathodic protection in natural environments.

   e. That any relatively lesser bonded area was caused by electrical stressing in combination with the elevated and or depressed temperature and was not attributable to an anomaly in the application process. Ability to resist disbondment is a desired quality on a comparative basis, but most insulating materials will disbond to some extent under the accelerated conditions of this test. Bond strength is more important for proper functioning of some coatings than others and the same measured disbondment for two different coating systems may not represent equivalent loss of corrosion protection.

   f. The amount of current flowing in the test cell may be a relative indicator of the extent of areas requiring protection against corrosion; however, the current density appearing in this test is much greater than that usually required for cathodic protection in natural, inland soil environments.

   g. Test voltages higher than those recommended may result in the formation of chlorine gas. The subsequent chemical effects on the coating could cast doubt on the interpretation of the test results.

Equipment Requirements

1. *Test Vessel*—A suitable nonreactive vessel shall be used, capable of withstanding internal heating at not less than 90°C and suitable for continuous circulation of the electrolyte.

   a. A19-L (5-gal) cylindrical glass vessel has been found suitable, having an approximate diameter of 300 mm (12 in.) and a depth of 300 mm. A flat bottom is required for operation of a magnetic stirring rod. An alternate means of heating the test sample can be provided by internally heating. The pipe sample may be filled with a suitable heat transfer material (oil, steel shot, etc). A thermocouple or thermometer and heater can be immersed in the heat transfer medium to effectively control the temperature of the sample. Dimensions of the vessel shall permit the following requirements:

      i. Test specimens shall be suspended vertically in the vessel with at least 25 mm (1 in.) clearance from the bottom.

ii. Test specimens shall be separated by not less than 38 mm (1⁄2 in.), and a vertically suspended anode can be placed at an equal distance from each specimen not less than the separation distance.

iii. Test specimens shall be separated from any wall of the vessel by not less than 13 mm (1⁄2 in.).

iv. Depth of electrolyte shall permit the test length of the specimen to be immersed as required.

v. The reference electrode may be placed anywhere in the vessel, provided it is separated from the specimen and from the anode by not less than 38 mm (1⁄2 in.).

2. *Anode*—The anode shall be provided with a factory sealed, insulated copper wire lead.

3. *Connectors*—Wiring from anode to test specimen shall be 4107 cmil (14-gage Awg), minimum, insulated copper. Attachment to the test specimen shall be by soldering or brazing to the non-immersed end, and the place of attachment shall be coated with an insulating material. A junction in the connecting wire is permitted, provided that it is made by means of a bolted pair of terminal lugs soldered or mechanically crimped to clean wire ends.

4. *Holiday Tools*—Holidays shall be made with conventional drills of the required diameter. For use in preparing small-diameter pipe specimens such as 19-mm (3⁄4-in.) nominal diameter pipe, the use of a drill modified by substantially grinding away the sharp cone point has been found effective in preventing perforation of the metal wall of the pipe. A sharp-pointed knife with a safe handle is required for use in making physical examinations. *Note - This aspect will not be implemented unless the coating does not demonstrate disbondment within the allotted test time.*

5. *Multimeters*:

a. *Multimeter*, for direct current, having an internal resistance of not less than 10 MV and having a range from 0.01 to 5 V for measuring potential to the reference electrode.

b. *Multimeter*, for direct current, having an internal resistance of not less than 11 MV and capable of measuring as low as 10 μV potential drop across a shunt in the test cell circuit.

c. *Multimeter*, for initial testing of apparent coating resistance. For these evaluations a four pin Wenner Test or a TREK meter will be used.

6. *Reference Electrode*—Saturated Cu CuSO4 electrode having a potential of −0.316 V with respect to the standard hydrogen electrode shall be the standard of reference in these test methods. Other electrodes may be used but measurements thus obtained shall be converted to the Cu CuSO4 reference for reporting by making the proper correction.

Note: See Appendix D for an explanation of reference cell conversions.

7. *Thermometers*, two, mercury-filled type, accurate to ±1°C. One shall be of the full-immersion type for measuring temperature near the bottom of the vessel, and a second thermometer shall be of the partial-immersion type for measuring temperature near the top of the vessel. *Note – Because of the test configuration the electrolyte temperature will be monitored at the heater/chiller.*

8. *Combination Heater Plate*, with built-in magnetic stirrer, or equivalent, shall be used for heating and stirring the electrolyte. The heater shall be adjustable to produce and control a temperature of 60 ± 1°C in the test vessel. *Note – An immersion heater is installed within the test specimen and the canola oil is kept at 93°C ± 5°C. A heater/ chiller is used to circulate the electrolyte (3% Sodium Chloride) and keep the test cell at 7°C ±.2°C. This provides a thermal gradient representative of a pipe type cable installation with the associated thermal stresses in the coating system.*
9. *Direct-Current Rectifier*, capable of supplying constant current at a voltage of 1.50 ± 0.01 V, as measured between the specimen and reference cell.
10. *Thickness Gage*, for measuring coating thickness in accordance with Test Method ASTM G 12[2].
11. *Precision Resistor*, 1V ± 1 %, 1W (min), to be used in the test cell circuit as a shunt for current.
12. *Carbon or Stainless Steel Electrode*, used temporarily with the volt-ohm-meter to determine apparent initial holiday status of the test specimen.
13. *Additional Connecting Wires*, 4107 cmil (14-gage Awg), minimum, insulated copper.
14. Brass Studs, used at a terminal board, together with alligator clips or knife switches, for making and breaking circuits. Note - Alligator clips shall not be used to connect the electrodes or specimens at the top location of test cells.

Reagents and Materials

The electrolyte shall consist of potable tap water or higher purity water (distilled or de-mineralized water is satisfactory).

Optional – addition of 1 weight % of each of the following technical-grade salts, calculated on an anhydrous basis: sodium chloride, sodium sulfate, and sodium carbonate.

Note – The resulting solution has a pH of 10 or higher and a resistivity of 25 to 50 V·cm at room temperature (a substitution of 3% Sodium Chloride or simulated seawater per ASTM D1141 - 98(2008)[10].

1. Materials for sealing the ends of coated pipe specimens may consist of bituminous products, wax, epoxy, or other materials, including molded elastomeric or plastic end caps, capable of withstanding the test temperature.
   Note – The sealing compound selected for the test cell was a silicone caulk that will withstand the elevated temperatures.
2. Plywood has been found suitable for the construction of nonconductive test vessel covers and for the support through apertures of test specimens and electrodes. Wood dowels introduced through holes in the top ends of test specimens have been found suitable for suspending test specimens from the vessel cover (see Figure 5-1).

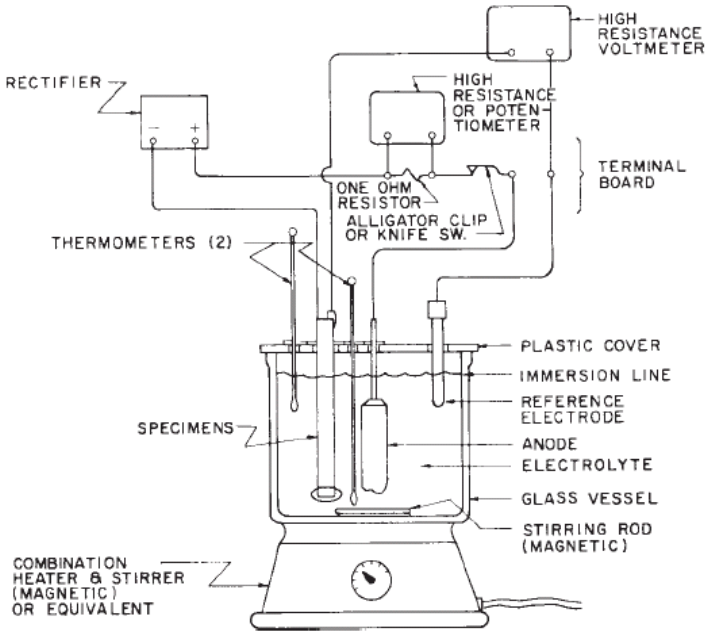


Figure 5-1
Cathodic disbondment test set-up per modified ASTM G42

Two test spools have been prepared to develop a methodology for insertion of coating disbondments into pipe type cable systems. This methodology includes environmental parameters that would normally induce the formation of a holiday but also have the test specimen to lose its coating adhesion and form a hidden corrosion cell beneath the coating surface. Figure 5-2 illustrates the apparatus required to insert a hidden corrosion cell beneath a disbonded coating.

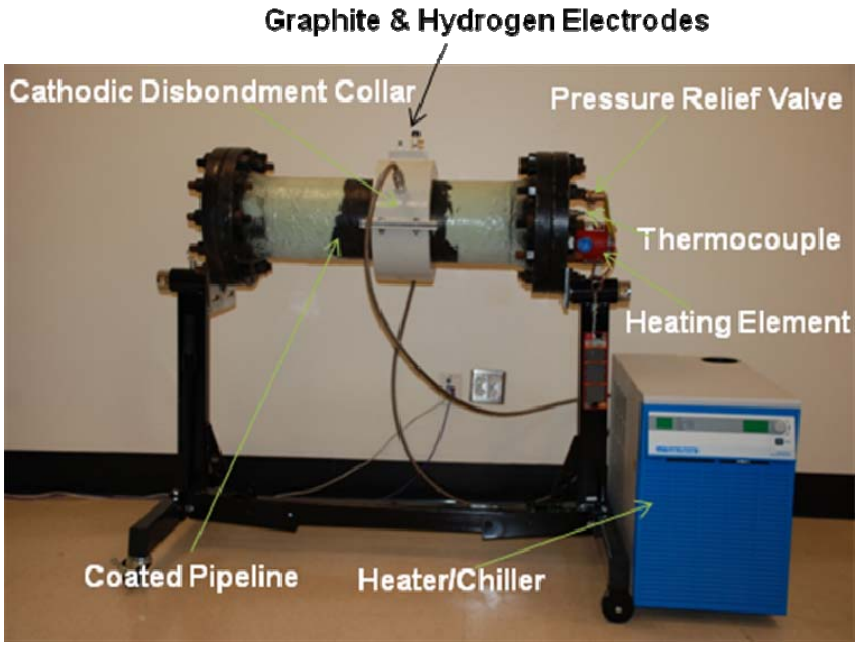


Figure 5-2
Coating disbondment test jig for development of hidden corrosion cells

Cathodic Disbondment Procedure

1. Immerse the test specimen in the electrolyte and connect it to the graphite anode as shown in Figure 5-1. Adjust the rectifier or voltage divider so that the potential between specimen and reference cell is −1.50 ± 0.01 V at 25°C (−1.53 ± 0.01 V at 93°C). The holiday may be positioned facing the anode or facing away from the anode as described in Test Methods ASTM G 8[1]. Space the anode with respect to test specimens as required. *Note – addition of electrolyte will be needed at the heater/ chiller unit.*
2. When using the electrolyte heating methods the temperature of the electrolyte surface to bottom shall be not less than 93°C. The electrolyte shall be continuously circulated by means of the heater/ chiller. The maximum temperature shall be attained 4 ± ½ h after starting the heater and immersing the specimen.

Note – Throughout the test period, ejected sealant or salt deposits, or both, may form near, or partially obstruct the intentional coating holiday. No attempt shall be made to clear the holiday while the test is in progress.

Electrical Monitoring Schedule

1. Electrical measurements shall be made on the start-up day and on each normal working day thereafter for the duration of the test.

Figure 5-3 illustrates the heater chiller, thermo controller and power supply. The power supply was set for 2.4 volts and the E2 voltage was 1.510 volts. The system was programmed to shut down after a specific time interval and the test spool would cool down to ambient temperature while the heater chiller would maintain a constant 7.2 degrees Celsius (19°C shown) within the test annulus.

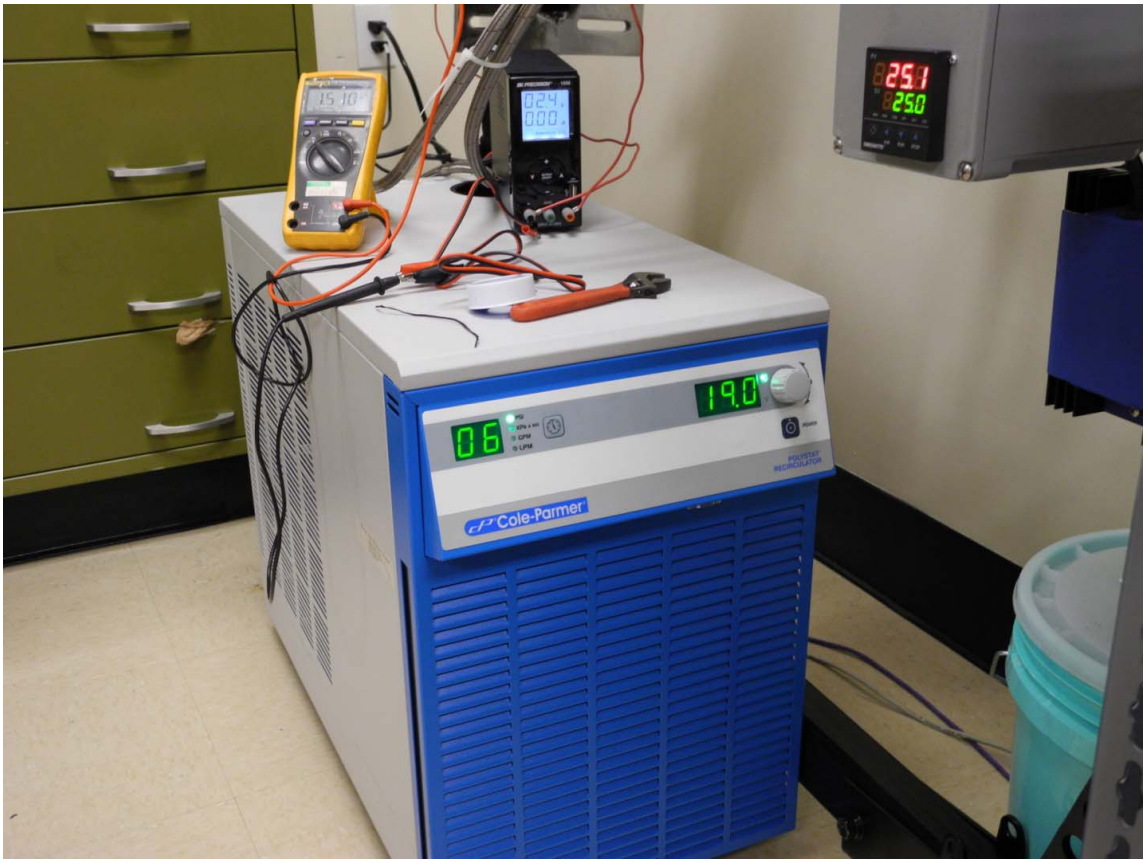


Figure 5-3
Illustrates the power supply, thermal controller and heater chiller

2. Electrical measurements and adjustments made each normal working day:

   a. Measure *E*2, the stress potential in volts between the test specimen and the reference electrode, without disconnecting the energized anode or specimen from the circuit. Use the high-resistance voltmeter described in the equipment section 5. The stress potential, *E*2, should measure − 1.50 ± 0.01 V at 25°C (−1.53 ± 0.01 V at 93°C); if it does not, adjust the rectifier or voltage divider accordingly.

   b. After *E*2 has been measured and adjusted, if necessary, measure *I* 1, the current demand in amperes, by determining the potential drop across the 1-V precision resistor permanently installed in the test cell circuit with the high-impedance voltmeter. The voltage reading will be numerically equal to amperes.

Note – An alternative method of measuring current demand utilizes a zero-resistance ammeter. In this method, the wire connection between the test specimen and anode is temporarily broken and a zero-resistance ammeter temporarily interposed between the specimen and the anode. Reconnect the specimen to the anode with the connector wire as soon as this measurement is completed.

c. Measure *E*1, the polarized potential, in volts, using the high-impedance voltmeter connected between the test specimen and the reference electrode as follows:

i. Disconnect the anode from the test specimen while closely observing the high-resistance voltmeter. As the instrument pointer falls, it will dwell significantly at the polarized potential before recording further. The dwell point is *E*1.

3. Standard duration of the test period shall be 30 days (720 h) in the energized test vessel including warm-up and cool-down times, unless longer test periods are specified.
4. A physical examination shall be performed immediately upon termination of the test period as follows:

a. Before examination, wash the test specimen carefully under gently flowing tap water without disturbing visible destructive effects. Adjust the temperature of the tap water so that it approximates that of the room temperature.

b. Examine the entire immersed area visually for any evidence of new holidays and loosening of coating at the edge of all holidays.

c. Determine if the coating has been loosened at the immersed test section by ultrasonic inspection.

d. Measure the disbonded area and outline the area with a permanent marker.

Note – The use of a transparent film having a grid laid out in small squares such as 2.54 mm (0.1 in.) on a side has been found useful. The film is placed against the unsealed area and the boundary of the unsealed area is traced on the grid. The area is then obtained by counting the squares within the bounded area.

e. Determine and record the resistivity and pH of the electrolyte at the beginning and end of the test period.

Test Considerations

1. Cathodic disbondment testing is typically used for below-grade coating systems.
2. The presence of pinholes, holidays, areas where the coating was applied too thinly or mechanical damage in the coating will accelerate cathodic disbondment.
3. Cathodic disbondment testing is not a suitable means for testing panels for zinc rich coatings, or coatings with other metallic loading, such as aluminum leaf or flake.

6
ELECTROCHEMICAL IMPEDANCE SPECTROSCOPY (EIS)

To evaluate coating systems in terms of their corrosion resistance and potential to degrade when exposed to corrosive test solutions, testing follows ASTM G106 – 89(2004) *Standard Practice for Verification of Algorithm and Equipment for Electrochemical Impedance Measurements[7]*. This standard practice provides a method to verify instrumentation and techniques for collecting and presenting electrochemical impedance data. Using this method, subtle coating changes can be detected and measured by monitoring the electrochemical behavior of a coating system.

EIS Overview

Initial EIS measurements are obtained on coated panels prior to accelerated exposure testing for a base line measurement. After the exposure period is complete, EIS measurements are again taken and then compared to the initial EIS measurements. The following coating properties can be determined by EIS:

- Capacitance
- Pore Resistance
- Moisture Absorption

When a coating is exposed to a test solution, a decrease in electrochemical impedance will be seen as a function of time. The decrease shows the breakdown and permeation of a coating by the test solution.

EIS evaluation exploits the changing frequency-dependent impedance of coatings during exposure testing to assess the degradation, permeability and water absorption of coatings. Non-conductive coatings that have not failed, will exhibit dominant insulative capacitive impedance. When coatings become permeated, penetrated, or absorb enough moisture to bridge from the exterior to the substrate metal, the resistance at low frequencies drops. It becomes bounded at the high end by the “pore resistance” or the equivalent electrical resistance in parallel with the capacitance of the coating.

Good coatings have high impedance—impedance is the ratio of the applied voltage to the current flowing and varies with the frequency of the applied voltage. Good coatings with high impedance allow very little current flow at low frequencies, which is critical because current flow is a key process in corrosion. Impedance considers:

- The dependence of an applied voltage signal on the frequency
- The phase shift between a sinusoidal applied voltage signal and the resulting current signal

Thus, both the “magnitude” and the “phase” are parts of the concept of impedance.

Traditional Test Setup

The test set up applies a sinusoidal voltage across the coating and measures the resulting currents. Both the ratio of voltage to current and the phase shift of the voltage are measured. A conductive metal substrate is used to make electrical contact to one side of the coating. To make contact with the other side, a glass vessel is sealed to the coating and filled with an electrolyte, a liquid capable of carrying current (see Figure 6-1).

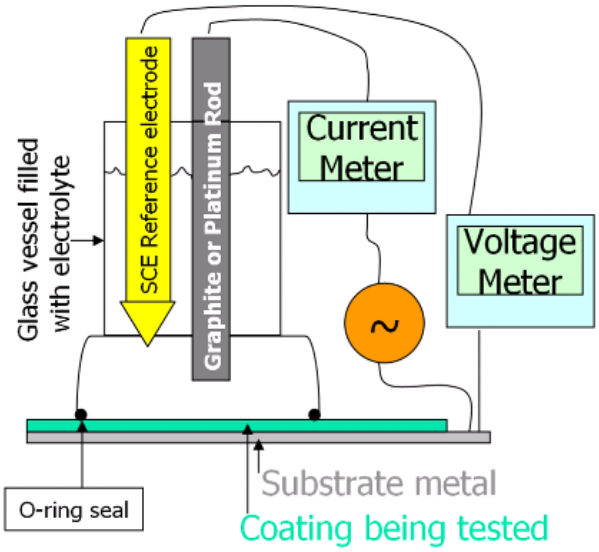


Figure 6-1
Test set-up for EIS testing

A computerized electrochemical system and EIS software are used to assist with data collection and analyses. A computer controls the voltage across the coating by injecting current through the platinum or graphite electrode in the electrolyte. The current and voltage are monitored continuously. Analysis of the resulting data yields the magnitude of the impedance and the phase between current and voltage. Measurement examples of EIS before and after hot acidic immersion exposure testing are shown in Table 6-1.

Table 6-1
Example of EIS measurements before and after hot acidic immersion exposure testing

Test ID	Time exposure to hot acidic chloride immersion (hours)	Percentage of initial protection	Capacitance (pF)	Pore resistance (Rp, 10^9ohm)	Water uptakes (vol. %)
Coating System A	0	100%	270	144.5	0
	336	95%	290	0.006262	1.6
Coating System B	0	100%	256	0.8	0
	336	94%	373	0.004013	9.1

Performance Criteria

EIS performance parameters for above and below-grade coatings after exposure are as follows:

1. Regardless to the exposure method (cyclic salt spray, immersion in hot acidic chloride solution, or exposure to corrosive soils), Testing protocol requires the following performance criteria:
   - Above-Grade Coatings — Maximal Impedance as observed at 0.1 Hz
     i. Good Coatings — > 108 ohms *cm^2
     ii. Rejected Coatings — < 108 ohms *cm^2
   - Below-Grade Coatings — Maximal Impedance as observed at 0.1 Hz
     i. Good Coatings — > 109 ohms *cm^2
     ii. Rejected Coatings — < 109 ohms *cm^2
2. If the impedance ratio does not change with time, one can conclude with a high degree of confidence that the coating is not altered and will perform well under actual service conditions.

Test Considerations

1. This test can also provide data for calculating permeation rate and minimum coating thickness and cure schedule requirements for adequate corrosion resistance.
2. This test method may not be appropriate for electrochemical impedance measurements of all materials or in all environments.

Graphical Interpretation of the Six Stages of Coating Degradation

Modeling the corrosion cell provides an understanding of the changes in each component and the time for each change to occur. The goal is that the exposure test can be correlated with real time and environmental factors.

a. RE = Reference Electrode

b. WE = Working Electrode (Control Sample)

c. Ru = Resistance of Electrolyte

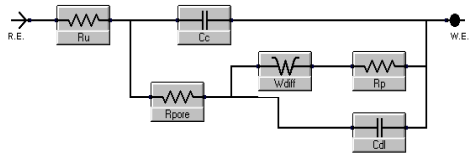
d. Rc = Resistance of Coating

e. Rp = Resistance of Electrolyte in Pore

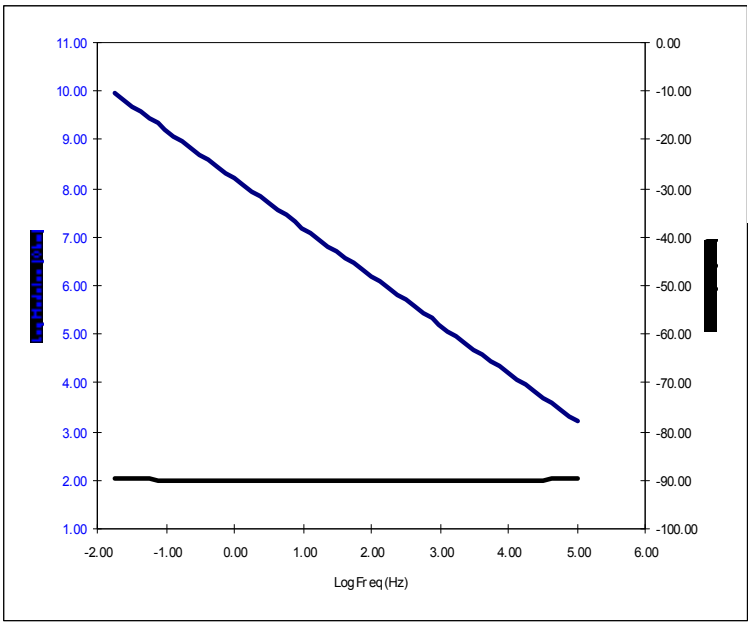
f. Wdif = Warburg Diffusion Coefficient

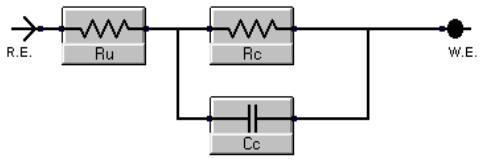
g. Cc = Capacitance of Coating

h. Cdl = Double Layer Capacitance (Corrosion Product)

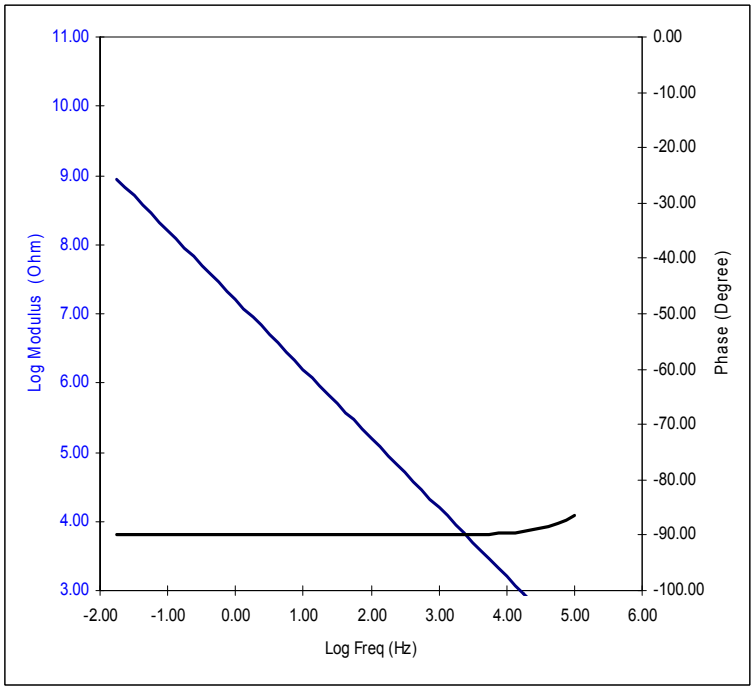


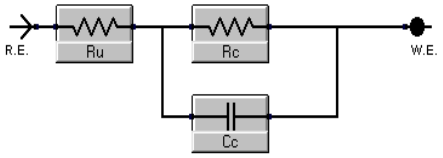
1. Purely Capacitive, Initial Immersion – Demonstrated by a 90° Phase Angle, -1 Slope in Impedance and a High Impedance at Low Frequency.



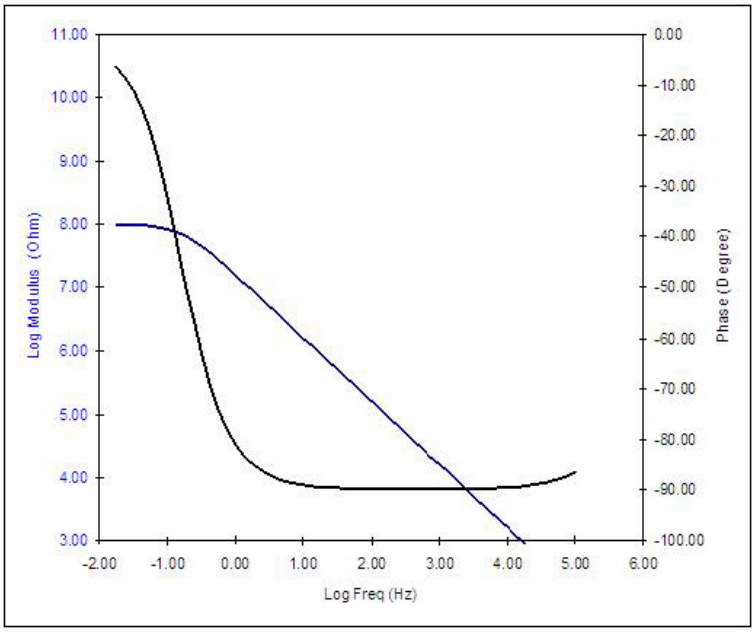


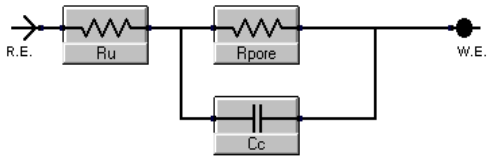
2. Absorption of Water – Demonstrated by a 90° Phase Angle, -1 Slope in Impedance and Lowered (shifted) Impedance at Low Frequency



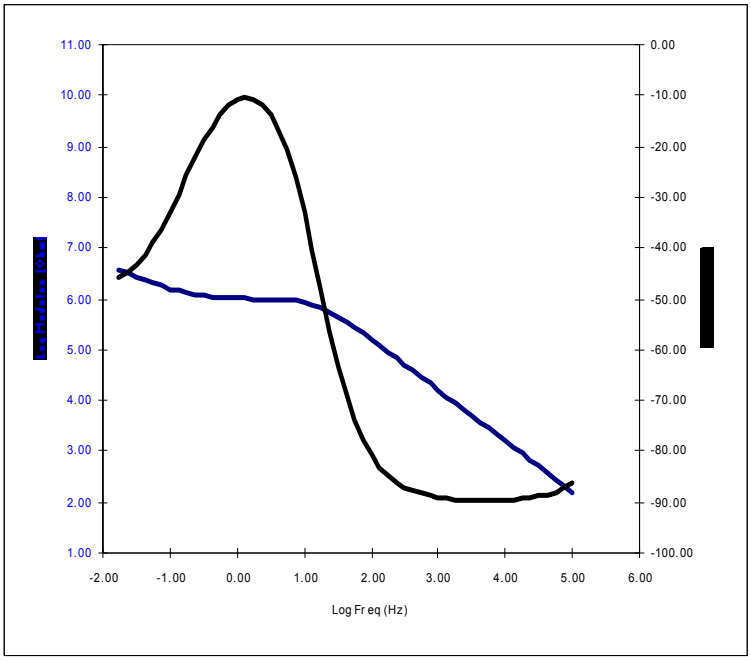


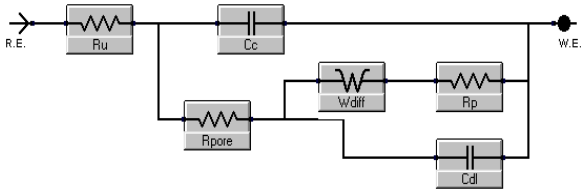
3. Development of a Pore Resistance – Demonstrated by a phase angle that is no longer constant and the Impedance Magnitude flattens off at low frequency.



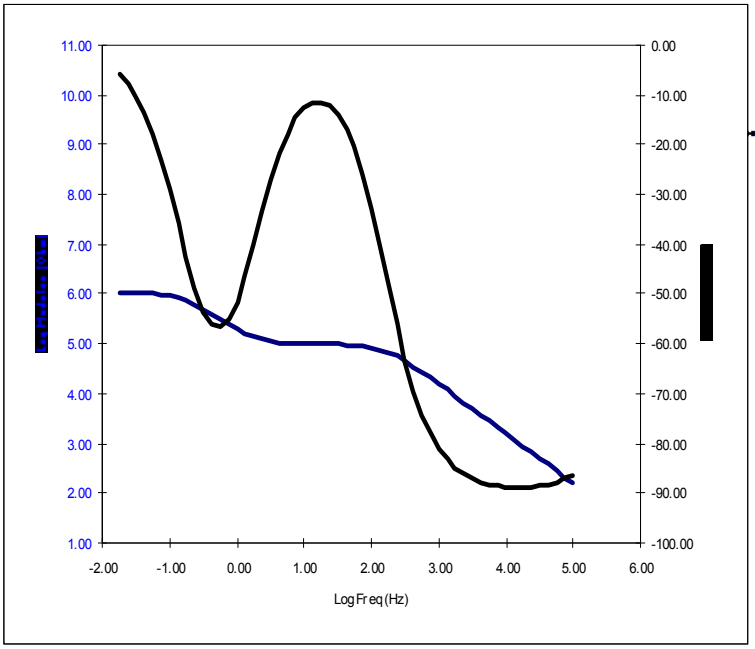


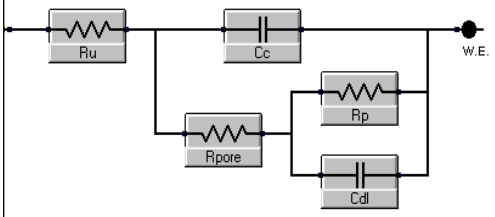
4. Diffusion Controlled Corrosion Through Pores – Demonstrated by phase angle shows two time constants and the impedance magnitude continues to decrease at low frequency.



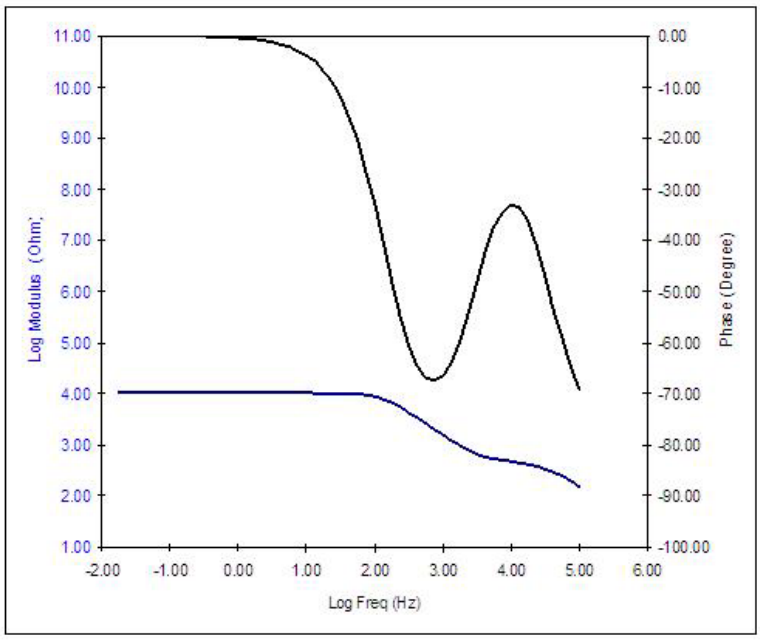


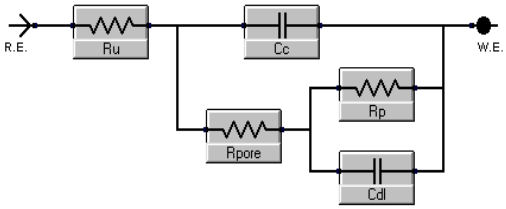
5. Target Stage - Free Corrosion During Blistering – Demonstrated by the phase angle showing two time constants and the impedance magnitude continues to decrease at low frequency.





6. Major Coating Damage – Demonstrated by the phase angle no longer is at –90^{o} at high frequency and the impedance magnitude has decrease six orders of magnitude during the experiment.





7
PASSIVE HALF CELL ASSESSMENT

Passive half cell measurements were evaluated to see if the changes could be trended as a screening process. The tests were made by connecting to the working electrode (pipe) through a voltmeter to a copper copper sulfate (Cu Cu SO4) half cell. The reference cell was then relocated along the grid to discern areas that may have disbonded.

The test results indicated that the coating was still considered a perfect barrier without discontinuities and would not allow a couple between the reference cell and the working electrode (pipe).

8
TEST DATA AND ANALYSIS RESULTS

Test Cell Visual Inspection

The test cell was dismantled and inspected for damage due to the exposure testing. The nitrile oring seals expanded in the glands making the disassembly difficult (Figure 8-1) and the graphite counter electrode fractured due to brittleness.



Figure 8-1
Disassembling the test cell for inspection was complicated due to the harsh test environment

The fasteners selected for assembly of the test cell were a stainless alloy and did not exhibit any corrosion. The test cell housings (see Figure 8-2) did have a significant amount of corrosion originating at the edges where coating systems are traditionally thinnest.



Figure 8-2
The test cell had indications of corrosion within the bolt pattern

Once the housing was removed from the pipe spool it was discovered that there was a significant amount of corrosion on the internal surfaces. The power coating system had developed discontinuities due to the thermal cycles and exposure to the cathodic disbondment sequences. All of the damage originated at the weld joints, test ports and the cooling cycle ports.

It was of interest that the corrosion products created a “staining effect” in the coating system and the flow patterns illustrated the boundry layers where the flow was laminar and areas that had reduced flow. The right side of the lower housing (Figure 8-3) shows the discharge or return port where the coolant was routed to the chiller for heat removal. There was some staining at that location and it appeared to be evenly distributed to either side.

The right side of the upper housing (Figure 8-3) was the inlet port to the test cell and had significant staining where there was corrosion originating within the port and housing edges. The staining followed the circumference of the housing into the lower housing before diffusing into an area of reduced flow where the weld seams developed discontinuities and subsequent corrosion. There was little weld seam corrosion damage within the upper housing except at the test ports where the reference cell and counter electrode were located. What is remarkable is that there is little if any corrosion at the edges of the housings where contact is made with the test cell.

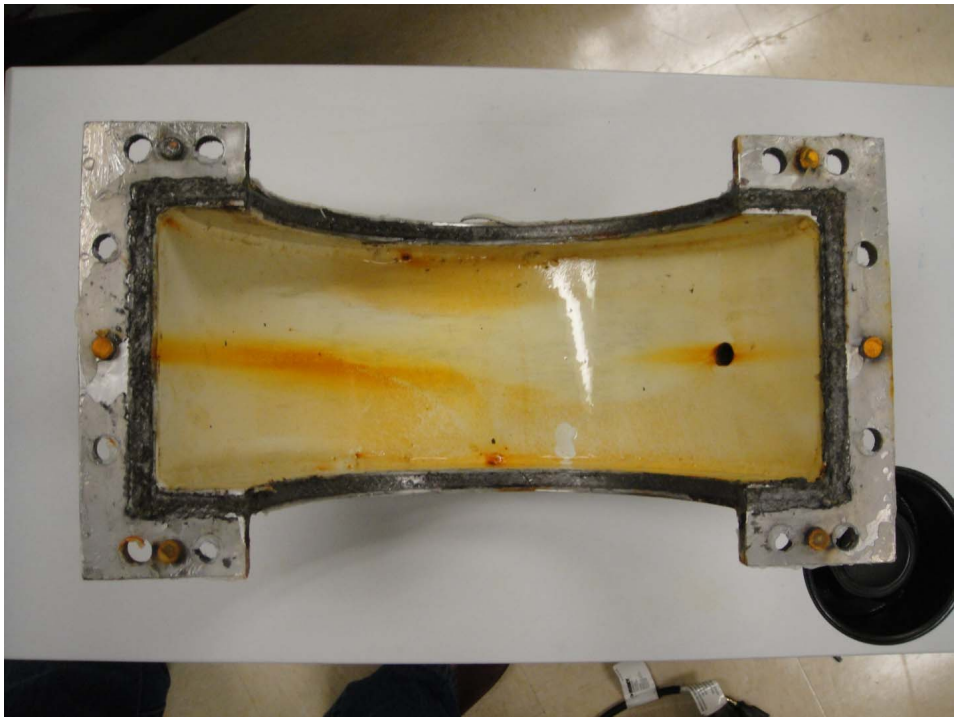


Figure 8-3
Lower housing of the test cell showing corrosion

Inspection of the upper housing also revealed that there was a significant amount corrosion within the instrumentation ports (see Figure 8-5). A design change will be made to lengthen the Teflon inserts with the hope that isolating the electrodes will eliminate current exchange the counter electrode (left).

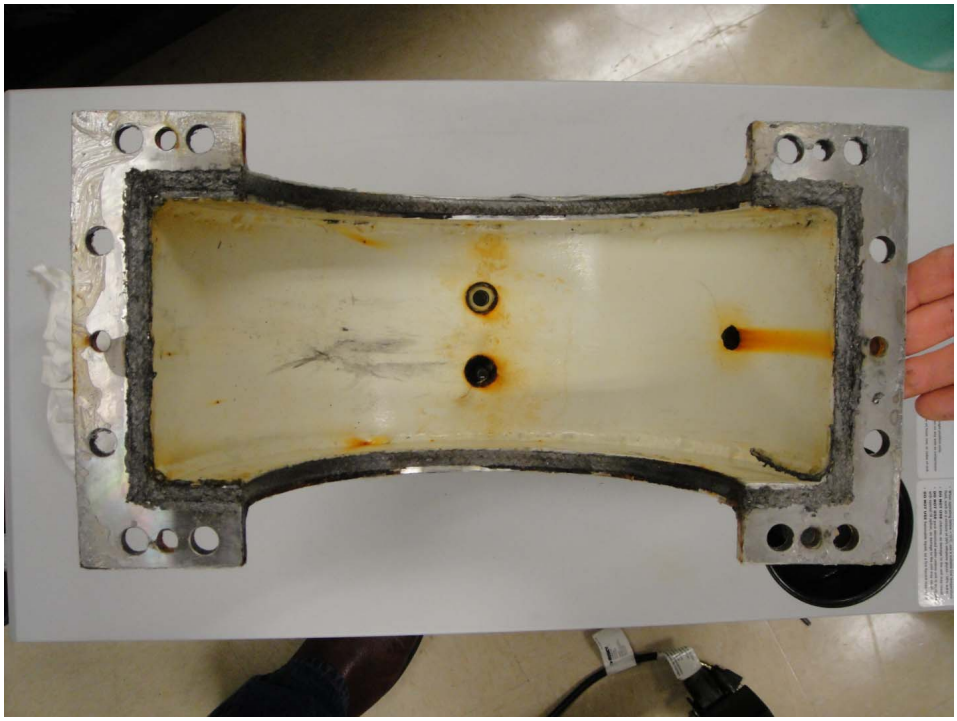


Figure 8-4
Upper test cell housing



Figure 8-5
Illustrates the corrosion originating at the test ports (counter electrode at left and reference electrode on right)

Cathodic Disbondment Data

During the 1200 hours of exposure time the test cell parameters were recorded for subsequent trending. Measurements were collected during the test while at elevated temperature (see Table 8-1) and then again when the system went back to ambient conditions (see Table 8-2). The test cell temperature was maintained through the exposure test to a constant 7.2°C while the coating system experienced the impact of the thermal load and the impressed current.

Table 8-1
Cathodic disbondment data during the elevated temperatures

Test Time	Elapsed Time (hrs)	Current	E1 (VDc)	E2 (VDc)	Oil (^{o}C)	Test Cell (^{o}C)
10/17/11 5:04 PM	75.2	2.9	1.056	1.462	90.0	7.2
10/24/11 8:51 AM	235.0	3.0	1.173	1.523	90.7	7.2
11/3/11 4:00 PM	482.2	3.7	1.456	1.549	92.0	7.2
11/4/11 4:00 PM	506.2	3.7	1.456	1.549	92	7.2
11/8/11 4:00 PM	602.2	4.0	1.451	1.553	92.0	7.2
11/9/11 4:45 PM	626.9	4.8	0.994	1.518	90.2	7.2
11/10/11 4:00 PM	650.2	1.4	0.895	1.468	93.8	7.2
11/14/11 4:38 PM	746.8	1.9	0.954	1.464	91.3	7.2
11/15/11 4:45 PM	770.9	2.3	1.225	1.532	86.9	7.2
11/17/11 4:00 PM	818.2	2.3	0.977	1.526	92.9	7.3
11/28/2011 16:50	1,083.0	4.0	1.272	1.54	80.6	7.2
11/29/2011 16:39	1,106.8	3.7	1.447	1.508	91.4	7.2
11/30/11 4:17 PM	1,130.5	4.4	0.997	1.528	56.7	7.2
12/1/11 4:25 PM	1,154.6	4.4	1.124	1.575	76.2	7.2

Table 8-2
Cathodic disbondment data during the ambient temperatures

Test Time	Elapsed Time (hrs)	E1 (VDc)	E2 (VDc)	Current	Oil (oC)	Test Cell (oC)
10/14/11 1:49 PM	0.0	n/a	n/a	n/a	22.0	22.0
10/25/11 9:23 AM	259.6	1.471	1.531	9.0	18.5	7.2
10/26/11 8:56 AM	283.1	1.117	1.565	9.0	18.1	7.2
10/27/11 8:52 AM	307.0	0.827	1.568	4.1	22.5	7.0
10/28/11 9:24 AM	331.6	0.863	1.504	5.0	18.9	7.2
10/31/11 8:56 AM	403.1	1.417	1.565	4.9	20.4	7.2
11/1/11 8:00 AM	426.2	1.367	1.534	4.8	18.1	7.2
11/4/11 8:10 AM	498.4	0.947	1.618	3.9	18.8	7.2
11/9/11 8:00 AM	618.2	1.051	1.540	3.9	16.9	7.2
11/10/11 8:00 AM	642.2	0.924	1.454	4.4	17.3	7.2
11/10/11 11:00 AM	645.2	0.999	1.517	1.4	17.6	7.2
11/11/11 8:00 AM	666.2	1.01	1.474	1.6	17.2	7.2
11/14/11 8:00 AM	738.2	1.005	1.549	1.8	16.8	7.2
11/16/11 8:00 AM	786.2	1.144	1.585	2.4	28.3	7.2
11/17/11 8:00 AM	810.2	1.146	1.51	2.1	23.8	7.2
11/18/11 8:00 AM	834.2	1.507	1.615	2.4	18.4	7.2
11/29/11 9:00 AM	1,099.2	1.034	1.577	3.4	23.7	7.2
12/1/11 8:40 AM	1,146.8	1.471	1.564	4.0	29.5	7.2
12/2/11 8:11 AM	1,170.4	0.934	1.538	4.1	29	7.2

Graphing the data from the heat cycle and cool down cycle illustrates that the current density requirement was highest at the beginning and end of the exposure testing. The polarization of the test pipe increased during the exposure test as shown in Figure 8-6 and decreased during the heat cycle as shown in Figure 8-7. The balance of parameters were unremarkable and demonstrated that the controls were maintained throughout the exposure testing.

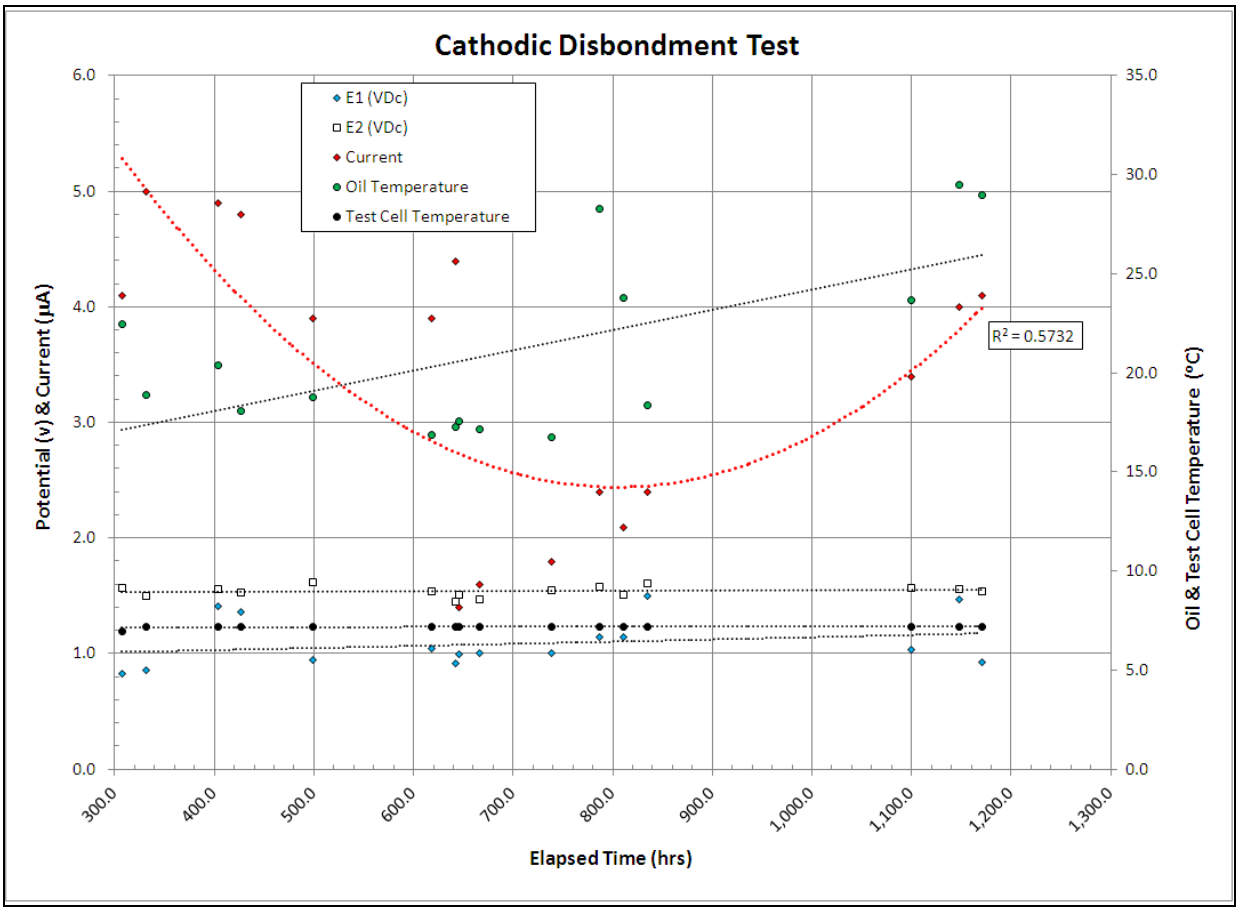


Figure 8-6
Cathodic disbondment data at ambient temperatures

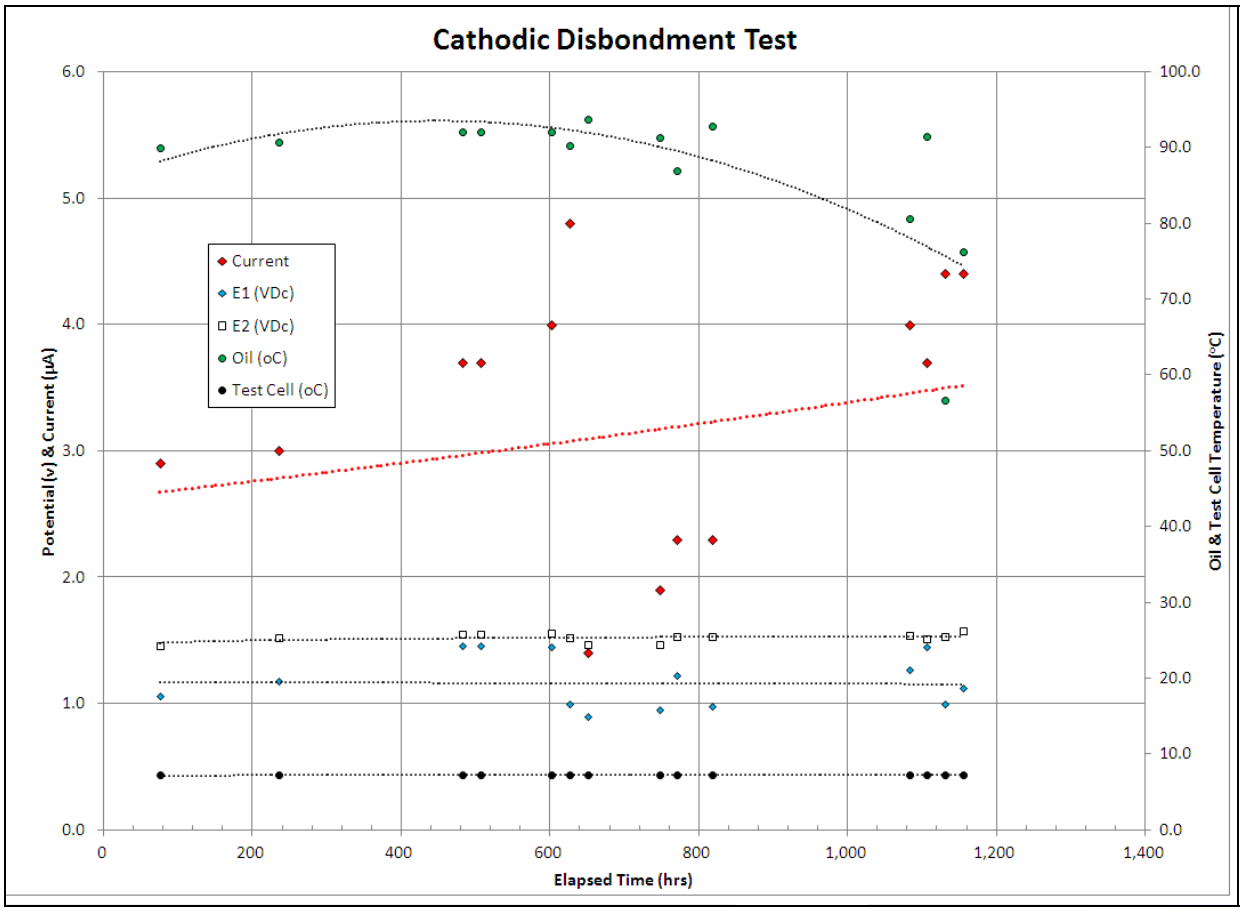


Figure 8-7
Cathodic disbondment data at elevated temperatures

The temperature in the laboratory was also monitored (see Figure 8-8) to understand if there were correlations with any anomalies noted. The ambient temperature did change significantly due to the heat cycle of the test bed however the chiller maintained a constant 7.2°C throughout the exposure testing.

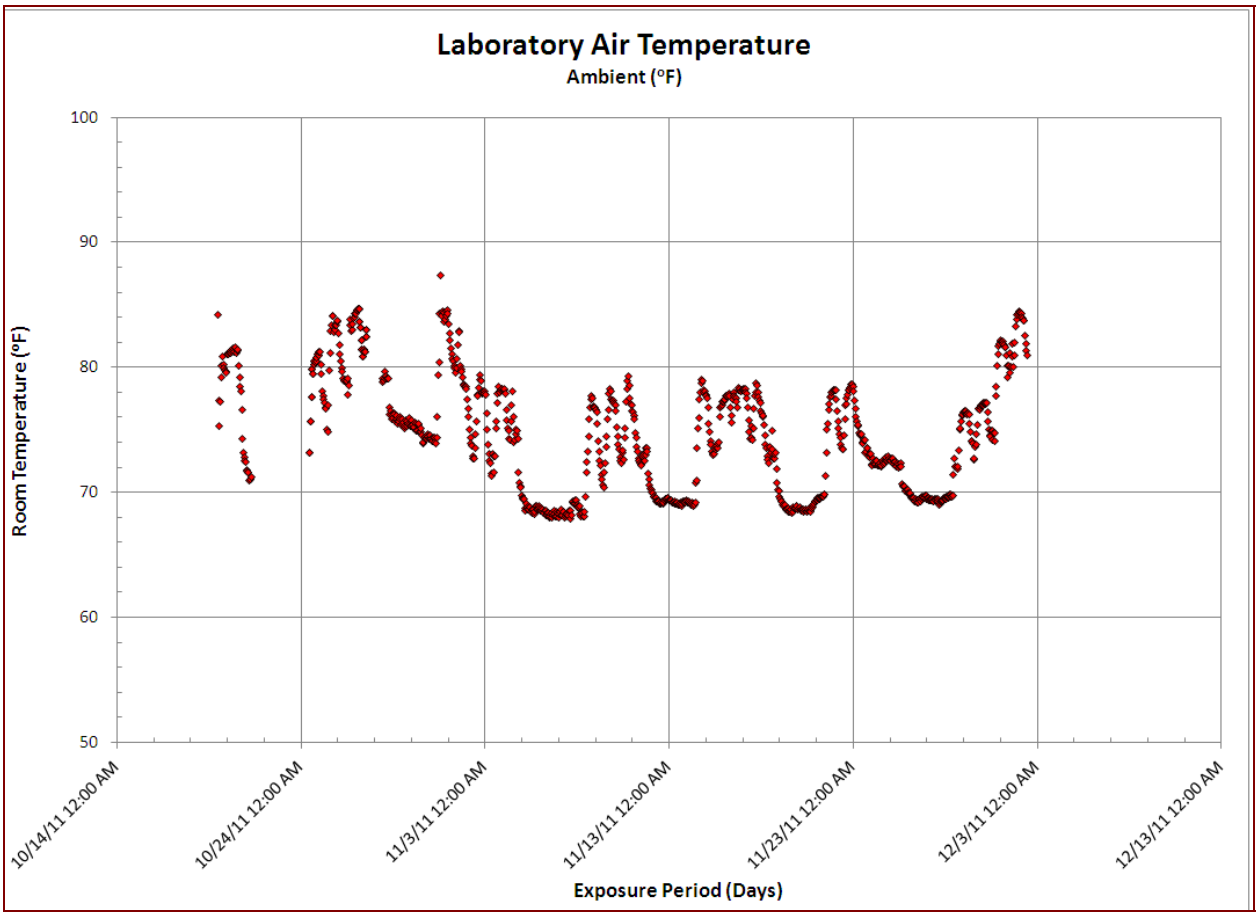


Figure 8-8
Ambient temperature changes within the corrosion laboratory

Ultrasonic Thickness Testing

An Olympus 38DL plus was used to measure the pipe wall in addition to the coating system thickness (see Figure 8-9 and Figure 8-10). The purpose of this test was not to have accurate thickness measurements but an indication where the adhesion properties for the coating system have changed. A single element transducer was selected that did not discriminate between the pipe wall and the coating thickness. The resulting data (see Table 8-3) highlights areas where the coating system has lifted from the pipe and there is an air gap which will not allow a signal to reflect back to the transducer.

The graph of the data (Figure 8-11) allows a better understanding of where the air gaps exist and where destructive adhesion testing will be completed after initial technology evaluations are completed. The surface of the pipe was scribed with a grid using a paint pen in 1 inch divisions around the circumference and 1 1/4 divisions along the axis of the pipe. The grid was framed by the sealing area to note the effects of shadowing by the housing but also provide a frame of reference for locating the initiation points of each disbonded area.



Figure 8-9
Mapping the thickness of the coating and pipe wall

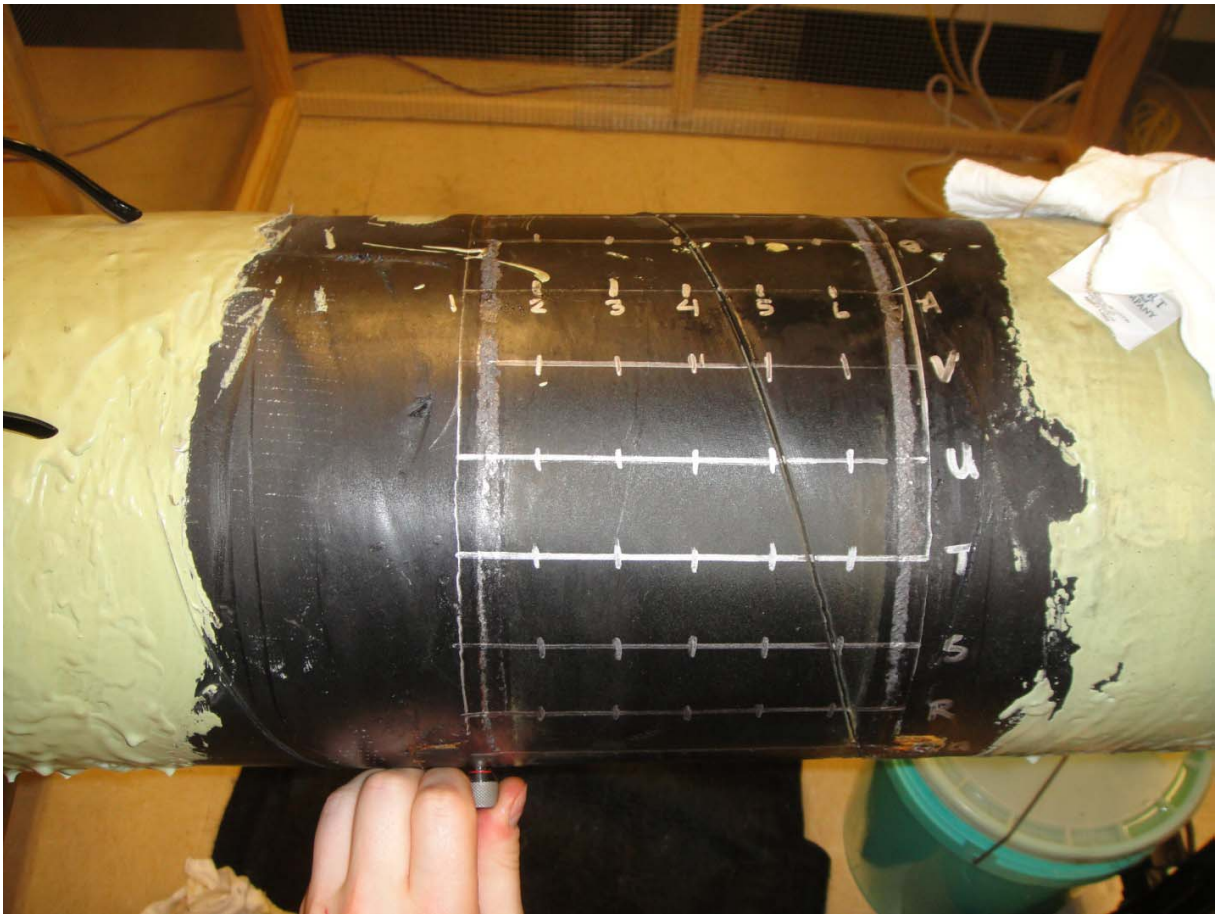


Figure 8-10
Mapping the disbondment area using a 1 in. x 1 1/4 in. grid

Table 8-3
Utrasonic thickness inspection data

		Pipe Axis (1 inch centers)						
		1	2	3	4	5	6	7
Pipe Circumference (1.25 inch centers)	A	0.149	0.459	0.153	0.442	0.552	0.249	0.204
	B	0.153	0	0.145	0.442	0.513	0.245	0
	C	0.153	0	0.444	0.518	0.515	0.237	0.136
	D	0.152	0.446	0.444	0.506	0.513	0.513	0
	E	0	0.448	0.215	0.215	0.221	0.437	0.138
	F	0.426	0.453	0.222	0.504	0.211	0	0.43
	G	0.437	0	0.229	0.219	0.49	0	0.131
	H	0.447	0	0.224	0.231	0.45	0	0.124
	I	0.443	0	0.244	0.238	0.454	0.475	0.174
	J	0.515	0.253	0.252	0	0	0	0.176
	K	0.23	0	0.251	0.445	0	0	0
	L	0.255	0	0.448	0.462	0	0	0
	M	0.535	0.546	0	0.45	0.18	0.471	0.18
	N	0.253	0.251	0.442	0.455	0.47	0.474	0
	O	0.247	0.235	0.45	0.183	0.469	0.478	0
	P	0.238	0	0.166	0.461	0.47	0.473	0.252
	Q	0.23	0	0.458	0.462	0.468	0	0.255
	R	0.181	0	0.462	0.468	0.462	0.471	0.242
	S	0	0	0.465	0.467	0.469	0.52	0.237
	T	0.156	0	0.466	0.464	0	0.265	0.247
	U	0.166	0	0.464	0.461	0	0	0.248
	V	0	0	0.455	0.458	0.25	0.241	0.242

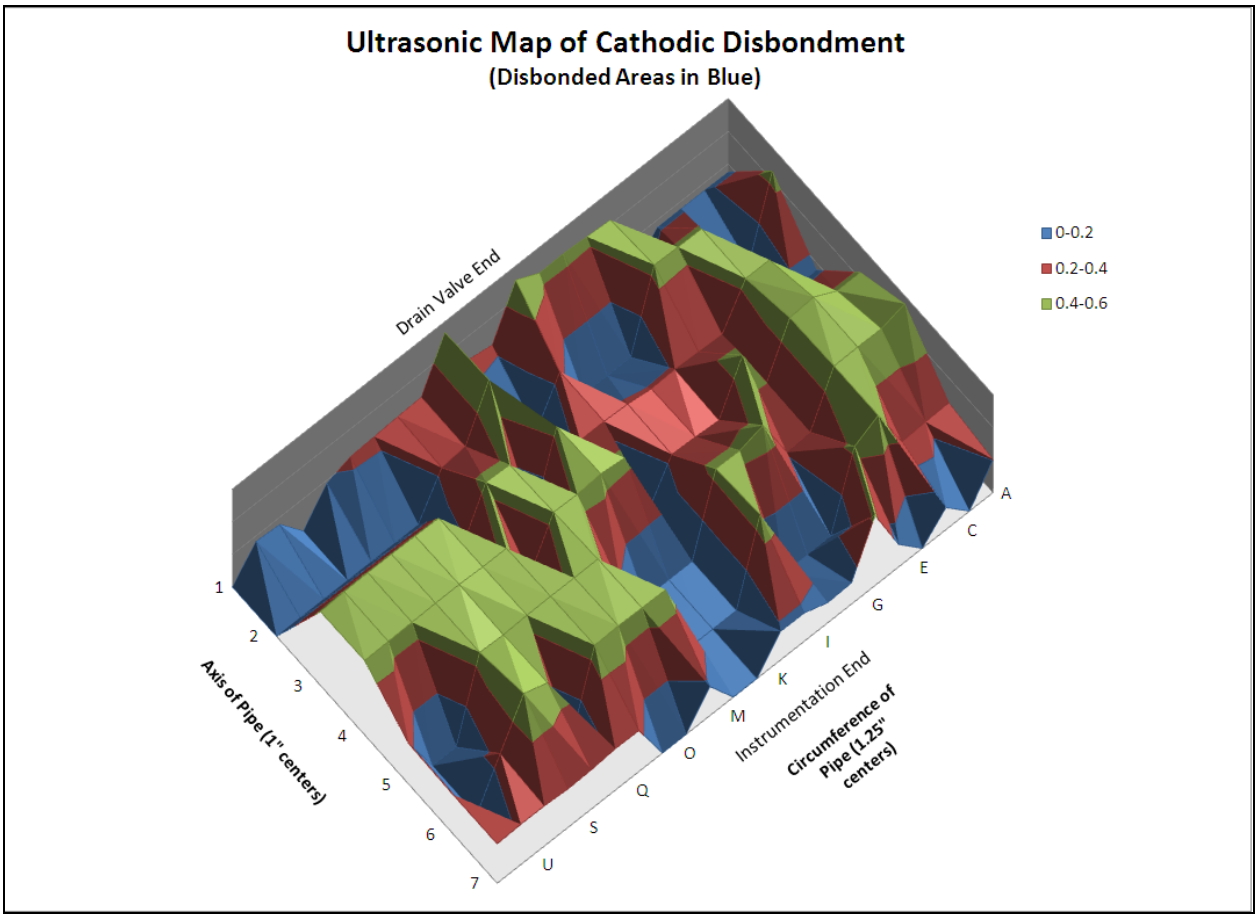


Figure 8-11
Graphical representation illustrating the ultrasonic thickness data

The disbonded areas are depicted by the dark blue depressions or valleys in the graph. The transitional areas of red are anticipated to have reduced levels of adhesion while the green are well adhered to the pipe surface.

Electrochemical Impedance Spectroscopy (EIS)

At the beginning of the EIS sequence the open circuit potential was measured. As the testing progressed it was noted that the test spool was polarized equal to the input voltage of the cathodic disbondment power supply. The technician was then instructed to ground the working electrode (pipe spool) to earth ground to dissipate this charge before further EIS testing.

The first parameter that is measured in the EIS test sequence is the open circuit potential (Figure 8-12). This is an indication of the system stability and should show no anomalies or noise during this part of the test.

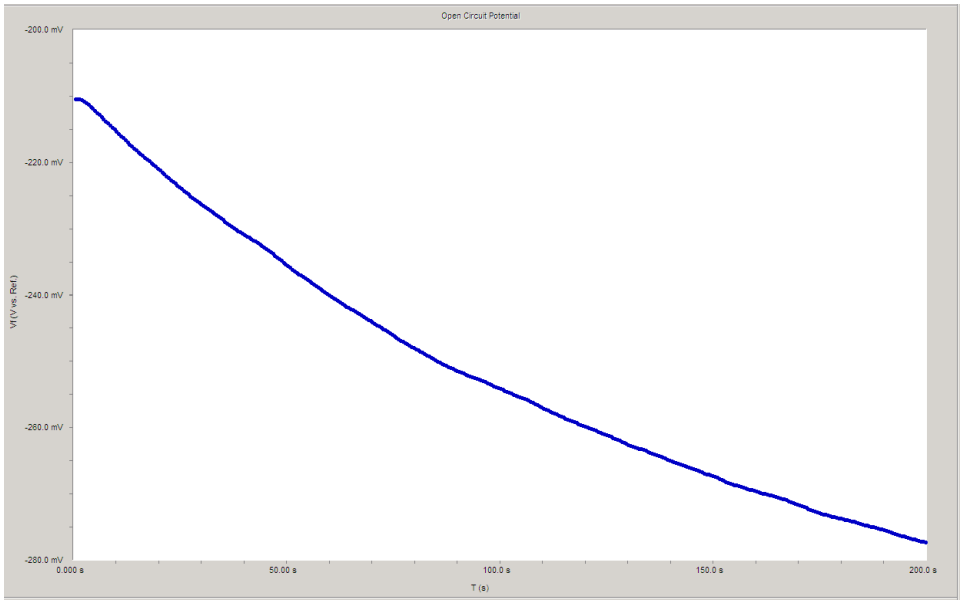


Figure 8-12
Open circuit potential (OCP) of the test spool before conducting the EIS test

The set up for the EIS testing included a conditioning period of 100 seconds before the OCP test was completed. The test sequence was run twice to understand the effects of the reference cell impedance and the data recorded in a table. Data analysis can be improved by inserting the solution (electrolyte) resistance into the model. The resistance of the test solution decreased during the exposure test from 787 ohms to 346 ohms. This was attributed to the iron oxide concentrations that were in solution due to corrosion product solubility (see Table 8-4).

Table 8-4
Water sample resistances

Water Source Characterization		
Water Origin	**Wenner Test (Ω-cm)**	**Trek Test (Ω)**
Distilled Water	610,000	200
Deionized Water	1,100,000	787
Tap Water	10,200	122
Test Water (1170 hrs)	-	346

The cathodic disbondment data was reviewed to understand when the adhesion properties may have started to diminish. The minimum current density levels were selected at about 810 hours of exposure time. Four analysis models were used to measure the impedance values but also to quantify the coating systems in terms of:

- Pore Resistance
- Coating Capacitance
- Faradaic (Polarization) Resistance
- Exposed Metal Capacitance
- Uncompensated Solution Resistance
- Corrosion (Double Layer) “Capacitance” (CPE)

These values are described in more detail in chapter 6 and each model is depicted in graphs Figure 8-13, Figure 8-14, Figure 8-15 and Figure 8-16. Figure 8-16 has the best goodness of fit (R2 = 0.2014) however each model has a significant amount of “noise” at the lower frequencies and these are traditionally of interest when evaluating a coating system to understand impedance. Because the OCP was unremarkable the thought was that there was still some source of this noise and it may be the test spool capacitance itself. The results of the four models can be compared in Table 8-5.

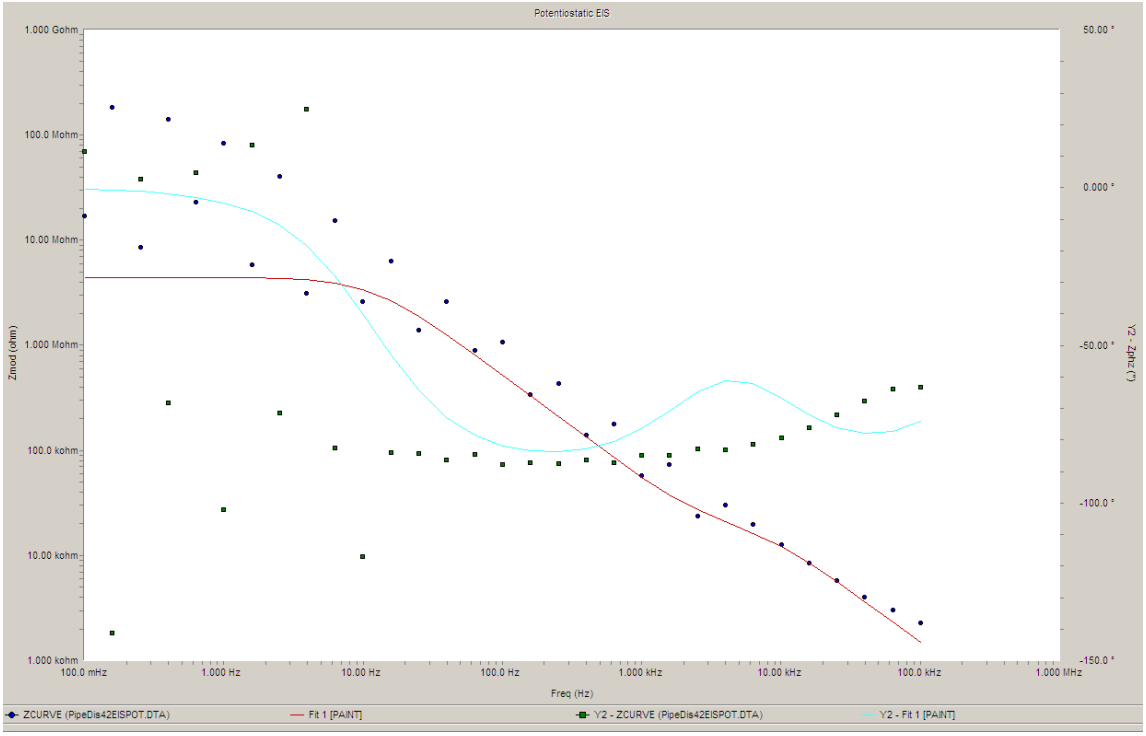


Figure 8-13
Levenberg-Marquardt Method using a traditional paint model

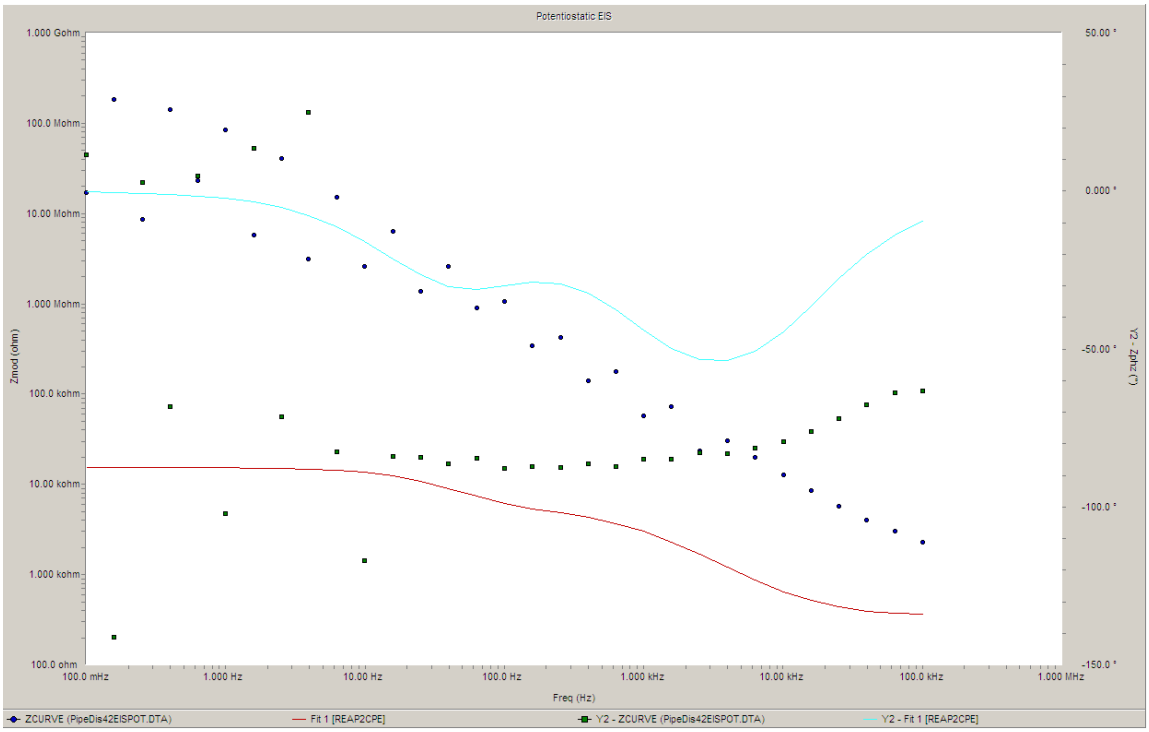


Figure 8-14
Levenberg-Marquardt Method using a rapid assessment model

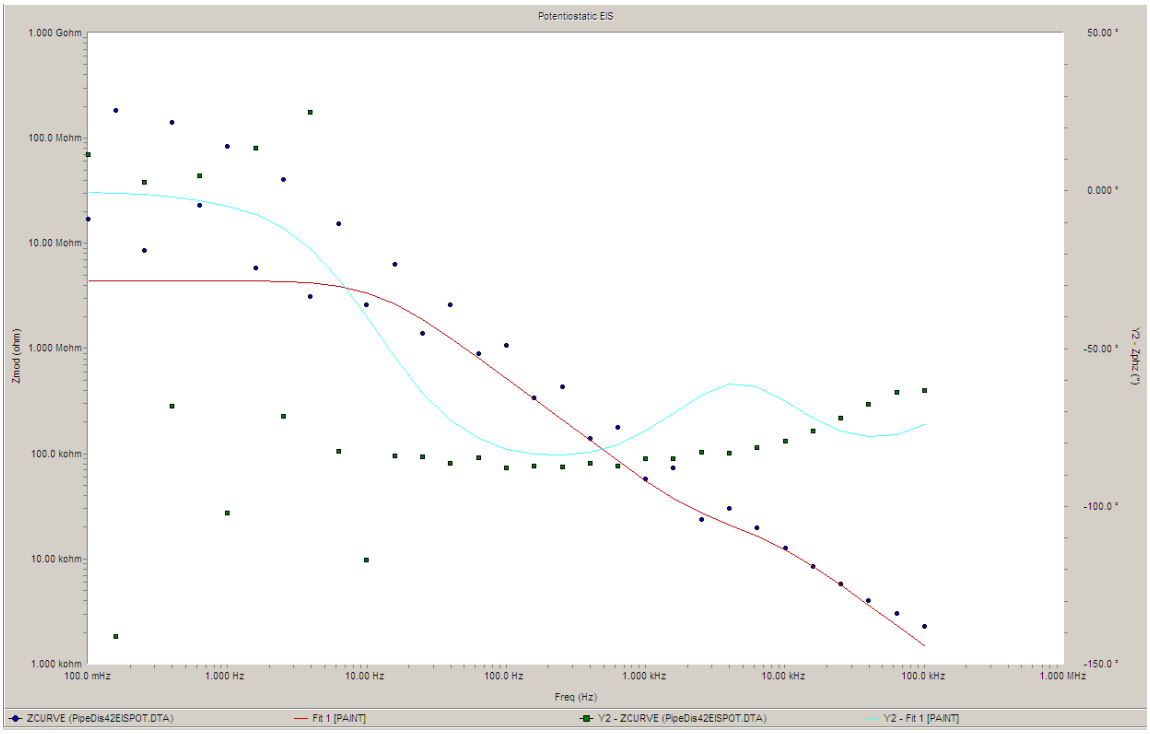


Figure 8-15
Simplex method using a traditional paint model

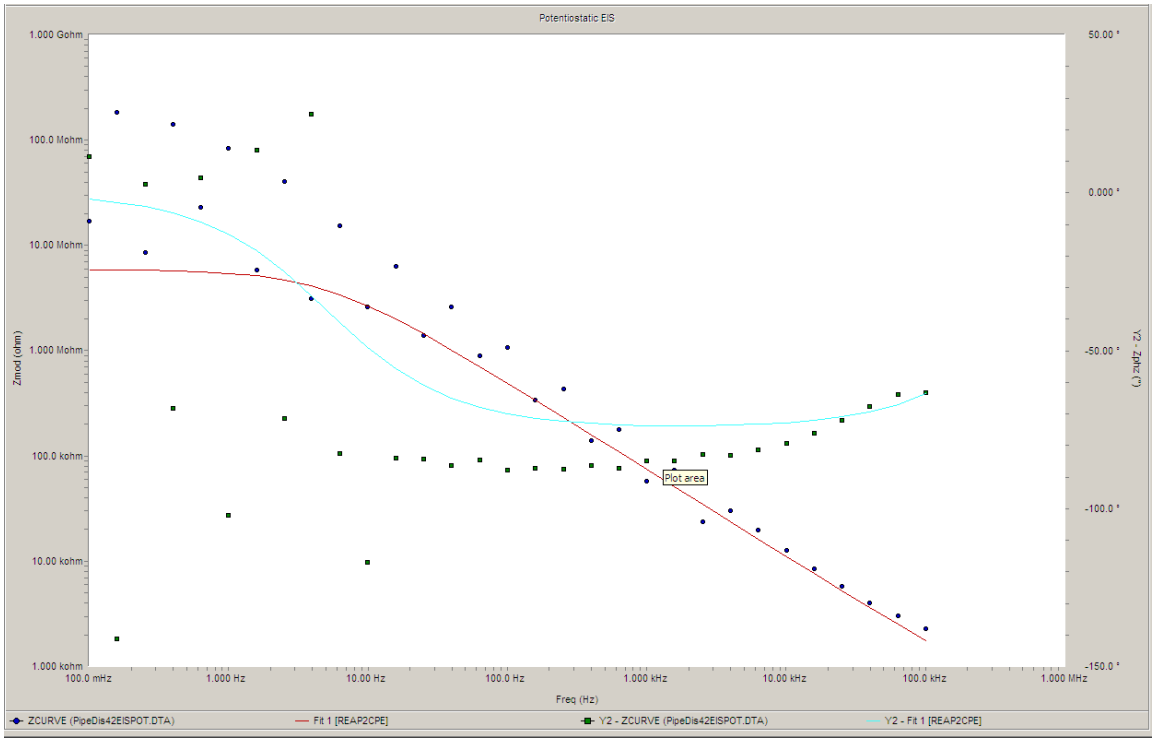


Figure 8-16
Simplex method using a traditional rapid assessment model

Table 8-5
Summary results for the four analysis methods utilized

Characteristic (@ 810 hours)	Variable Name	Levenberg-Marquardt Method – Paint Model	Simplex Method – Paint Model	Levenberg-Marquardt Method – Reap Model	Simplex Method – Reap Model	Units
Pore Resistance	Rpo	30,240	30,430	5,000	15,210	Ω
Coating Capacitance	Cc	0.000	0.000	0.000	1.10E-09	F
Faradaic (Polarization) Resistance	Rf	4,405,000	4,384,000	-	-	Ω
Exposed Metal Capacitance	Cf	0	0	-	-	F
Uncompensated Solution Resistance	Ru or Rsoln	346	346	346	346	Ω
Corrosion (Double Layer) "Capacitance" (CPE)	Ccor	-	-	0	3.15E-09	F
Corrosion Resistance	Rcor	-	-	10,000	1,272,000	Ω

9
CONCLUSIONS

EIS was anticipated to provide the strongest diagnostics throughout the exposure test and due to the system sensitivity extensive learning was completed during troubleshooting the test bed. The cathodic disbondment data contributed to the histogram for the initiation marker and the ultrasonic thickness measurements identified areas of interest for destructive testing after initial inspection evaluations.

Cathodic Disbondment Testing

The cathodic disbondment data demonstrated that the test spool did change because of the inflection in the current density with the initial and final current levels nearly the same. This indicates that cathodic disbondment testing will not provide discrimination between an aged and new coating system for this application. It will however be used as a marker in future laboratory disbondment tests in identifying the initiation of adhesion degradation.

Electrochemical Impedance Testing

Electrochemical impedance testing provided extensive learning about coating system response to harsh environments with soil stress, thermal loads and stray currents. EIS supports the following observations and results as illustrated in Table 9-1 and Figure 9-1.

Observations

- Solution resistance decreased
- Coating system capacitance changed very little
- Corrosion products resistance increased
- Pore resistance increased
- Corrosion products capacitance decreased

1. The solution resistance is the electrolyte that was pumped through the test cell by the chiller and changed as expected because of the ionic species concentration increase.
2. The corrosion products resistance increased while the corrosion products capacitance decreased and those two results seem to complement each other.
3. The coating pore resistance increased and that may the result of the thermal cycle or thermal expansion of the coating material causing the pores to close. What is not explained is the capacitance of the coating system remained relatively constant throughout the exposure testing.

Table 9-1
Electrochemical impedance spectroscopy results

Characteristic (810 hours)	Exposure Time (0 hrs)	Exposure Time (810 hrs)	Exposure Time (1,170 hrs)	Units
Rsoln	787	346	346	Ω
Rcor	18,020	1,272,000	4,234,000	Ω
Rpo	1,710	15,210	5,764,000	Ω
Ccor	9.59E-08	3.15E-09	6.483E-08	F
Cc	1.20E-09	1.10E-09	1.399E-09	F

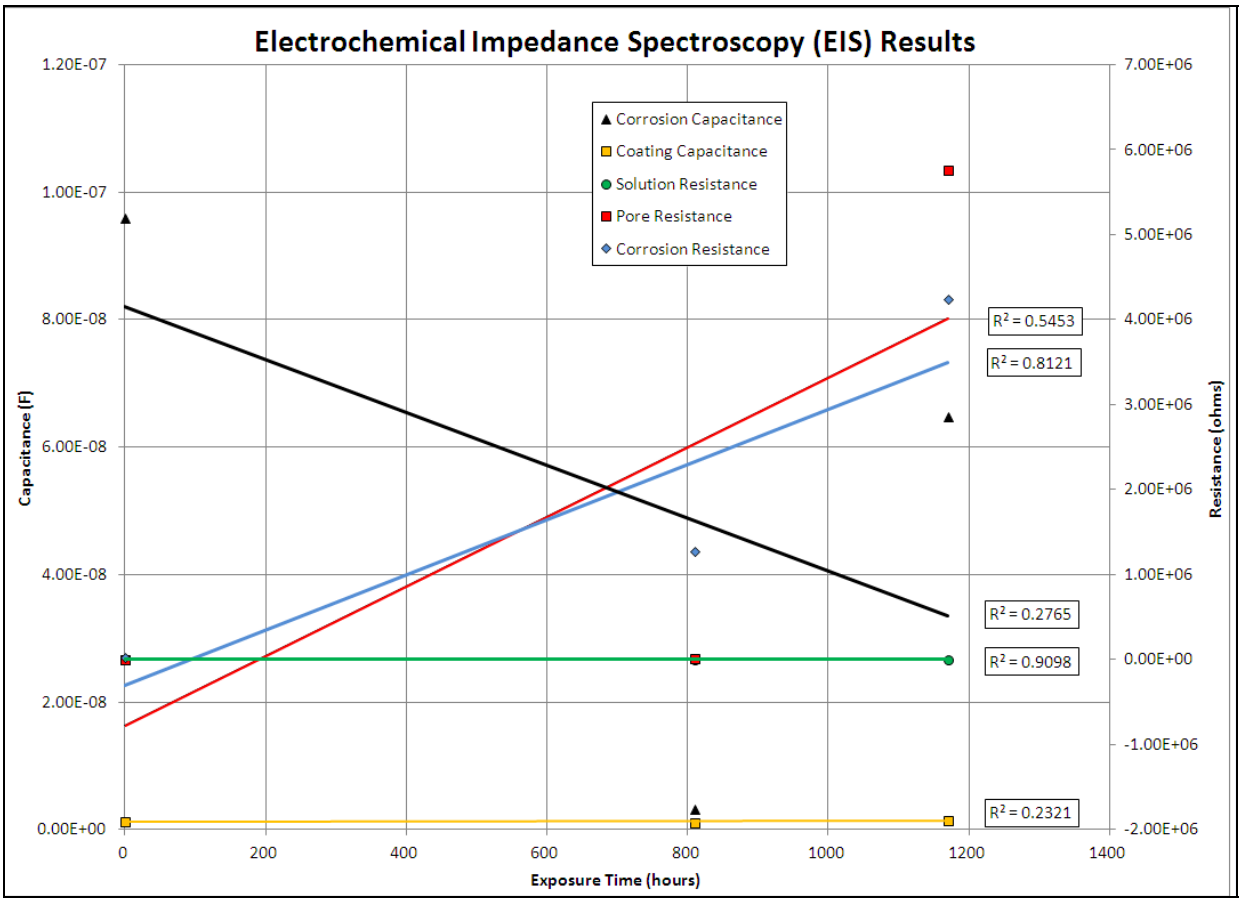


Figure 9-1
Graphical representation of EIS results

Ultrasonic Testing

The most conclusive results were achieved from ultrasonic thickness testing which demonstrated that the coating system suffered from adhesive failures in specific locations. It is anticipated that there will be areas within the grid map which have cohesive failures or reduced adhesion to the pipe surface (see Figure 8-11and Table 8-3). In Table 8-3 the cells with a null reading denote disbonded areas while Figure 8-11 illustrates locations in blue where the coating system has lost its adhesion to the substrate.

10
FUTURE WORK

The next phase of this project is to evaluate new and emerging technologies that have potential as a screening or predictive inspection technology or technique. A few existing test technologies have been identified that may locate disbonded coatings including guided wave techniques such as EMAT or MsS or impedance measurement techniques such as the EPRI Zed Meter. New electrochemical techniques such as Capacitance Decay Rate (CDR) will also be evaluated in the corrosion laboratory on the test spool flaws. Evaluation of these techniques will start in 2012 and the results appended to this technical update.

Once the results from the evaluations on the test spool have been analyzed the adhesion properties for the coating on the test spool will be measured using the standard ASTM D4541 [9]. This is a protocol that quantifies the adhesion properties of a coating system by pulling an aluminum dolly that has been glued to the coating surface. After the epoxy has cured for a specific length of time a hole saw cuts the coating system around the dolly circumference down to the pipe surface and the dolly is hydraulically lifted from the pipe. The tensile force is registered on a digital readout and the values are transferred to a spreadsheet for graphing in a 3D plot. A series of control sample measurements will also be made on the length of pipe remaining from the test spool construction. That control measurement average and the resulting adhesion values will determine the percentage adhesion loss and the adhesion graph will then be compared to Figure 8-11 to confirm locations.

Note: The test protocol for adhesion measurements has been outlined in Appendix C for reference.

Each inspection method can then be categorized as a predictive or screening technology before migrating to the next phase of evaluations on larger test specimens and additional environmental factors.

A
REFERENCES

1. ASTM G 8 – Test Methods for Cathodic Disbonding of Pipeline Coatings
2. ASTM G 12 – Test Method for Nondestructive Measurement of Film Thickness of Pipeline Coatings on Steel
3. ASTM G 42 – Test Method for Cathodic Disbonding of Pipeline Coatings Subjected to Elevated Temperatures
4. ASTM G 62 – Test Methods for Holiday Detection in Pipeline Coatings
5. ASTM G 80 – Test Method for Specific Cathodic Disbonding of Pipeline Coatings
6. ASTM G 95 – Test Method for Cathodic Disbondment Test of Pipeline Coatings
7. ASTM G106 – 89(2004) Standard Practice for Verification of Algorithm and Equipment for Electrochemical Impedance Measurements
8. ISO/FDIS 16773-2 – Electrochemical impedance spectroscopy (EIS) on high impedance coated specimens
9. ASTM D4541 - 02 Standard Test Method for Pull-Off Strength of Coatings Using Portable Adhesion Testers
10. ASTM D1141 - 98 – Standard Practice for the Preparation of Substitute Ocean Water
11. ASTM D5162 - 08 – Standard Practice for Discontinuity (Holiday) Testing of Nonconductive Protective Coating on Metallic Substrates, Test Method B

B
TEST BED COMMISSIONING PROTOCOL

Test Bed Commissioning and Data Collection Outline:

1. Corrosion Test Cell Leakage Test
    a. Fill test cell with distilled water
    b. Circulate water using the heater/chiller pump
    c. Check for leaks

2. Heating Circuit Leakage Test
    a. Fill pipe spool with distilled water
    b. Check for leaks

3. Heating Circuit Thermal Test
    a. Fill the pipe spool with canola oil
    b. Increase temperature in 5°C increments until 50°C is reached
    c. Hold 50°C for two hours and then shut down thermal cycle test
    d. Check for leaks

4. Corrosion Cell Electrochemical Impedance Spectroscopy (EIS) Test
    a. Connnect the potentiostat according to the diagram
    b. Run a baseline impedance measurement

5. Cathodic Disbondment Baseline
    a. TBD

6. EIS & CD measurements
    a. Results

C
COATING ADHESION TEST

Adhesion Testing per ASTM D4541 - 02

With direct tensile testing, a hydraulic pump device is used to lift a dolly or plug glued to the coating surface. The applied force that is required to remove the coating is measured at the point of disbondment. Failure, or disbondment, will occur at the weakest point within the system (glue, substrate/coating interface, or coating layers). The force required for disbondment is measured in pounds per square inch. This test method maximizes tensile stress of a coating system rather than the shear stress, which is measured by other forms of adhesion testing.

The location where disbondment occurs is an important aspect of adhesion testing that should be considered in coating system performance. If disbondment occurs at the substrate/coating interface or between coating layers, it is referred to as an adhesion failure. If disbondment occurs within a coating layer itself, it is referred to as a cohesion failure. In terms of corrosion protection to the substrate, it is preferable that a coating system disbond within the coating system itself or at the glue site rather than at the substrate/coating interface (see Figure C-1).



Table C-1
Examples of disbondment due to tensile testing

Adhesion Performance Guidelines per ASTM D4541 - 02

Adhesion testing performance parameters include:

1. In general, the following guidelines are recommended.
    - Below-Grade Coatings (dry and after exposure) 1000 PSI (and above)
    - Above-Grade Coatings (dry and after exposure) 800 PSI (and above)

Test Considerations per ASTM D4541 - 02

1. While adhesion testing is a very important aspect, it is not an absolute indication of coating system performance. The ability of a coating to adhere to a substrate is based on several factors that are beyond a coating system's characteristics including substrate cleanliness and application methods. Therefore, adhesion should be measured prior to (dry) and after exposure to corrosive media. The percentage change in adhesion is a very important parameter and should also be considered.
2. Coating manufacture's information and specifications should be consulted prior to testing.
3. Portable adhesion testing device instructions and specifications should be carefully followed to ensure accuracy in testing.
4. Replicate samples of each coating system should be used to compensate for variations between coated panels and conditions.

D
REFERENCE CELL DATA CONVERSIONS

This is a brief example for the curious reader to understand how conversions are made between reference electrode types. This does not explain conversion factors for the effects of other environmental factors such as moisture, temperature or stray currents.

1. A saturated Cu CuSO4 (CSE) electrode reading − 1.50 V at 25°C will read − 1.53 V at 60°C, a scale increase of 0.03 V.
2. A saturated calomel electrode (SCE) at 25°C is converted to Cu CuSO4 by adding − 0.07 V to the observed reading. Figure D-1 illustrated the differences in scale between reference electrode types.

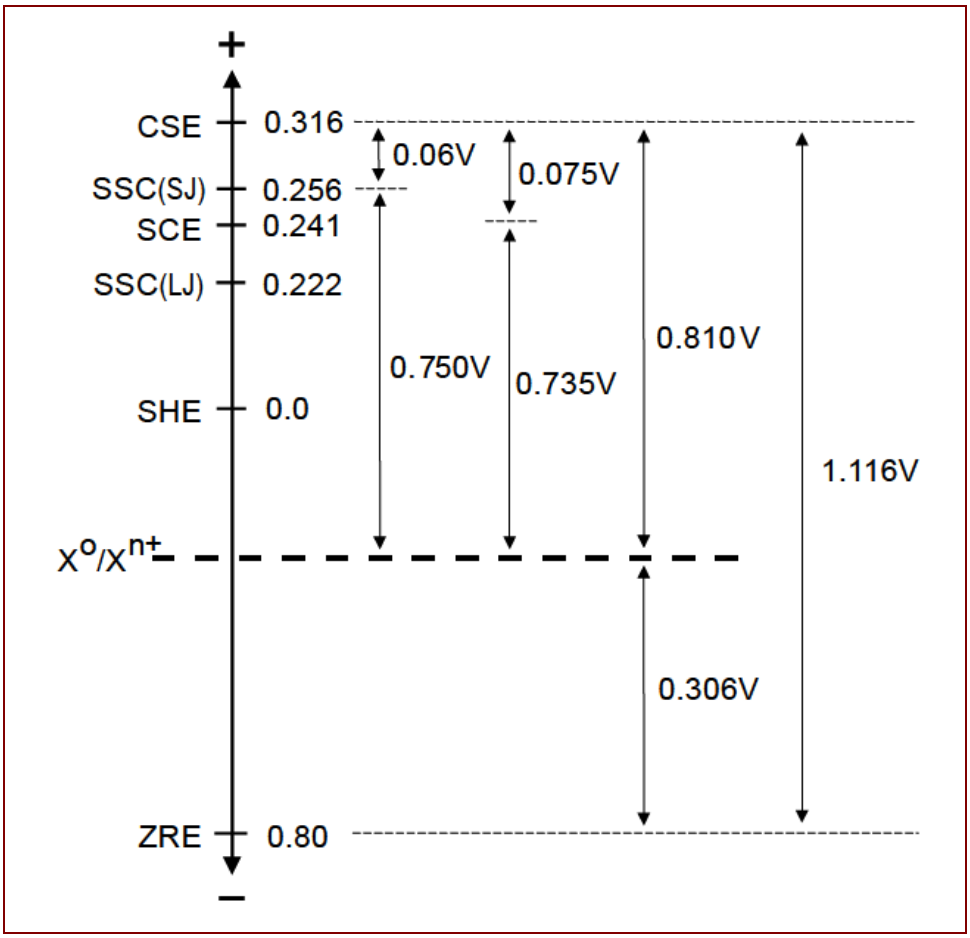


Table D-1
Conversion chart for different types of reference electrodes

3. If the saturated calomel electrode reads − 1.43 V at 25°C, it will read − 1.46 V at 60°C, a scale increase of 0.03 V.
4. It follows that a saturated calomel electrode reading of − 1.46 V at 60°C is equal to a saturated Cu CuSO4 reading of − 1.50 V at 25°C.
5. A 0.1 normal calomel electrode at 25°C is converted to Cu CuSO4 by subtracting − 0.02 V from the observed reading.
6. Since the potential change due to an increase from 25°C to 60°C is negligible, it follows that a 0.1 normal calomel electrode reading − 1.52 V at 60°C is equal to a saturated Cu CuSO4 reading of − 1.50 V at 25°C.

Export Control Restrictions

Access to and use of EPRI Intellectual Property is granted with the specific understanding and requirement that responsibility for ensuring full compliance with all applicable U.S. and foreign export laws and regulations is being undertaken by you and your company. This includes an obligation to ensure that any individual receiving access hereunder who is not a U.S. citizen or permanent U.S. resident is permitted access under applicable U.S. and foreign export laws and regulations. In the event you are uncertain whether you or your company may lawfully obtain access to this EPRI Intellectual Property, you acknowledge that it is your obligation to consult with your company's legal counsel to determine whether this access is lawful. Although EPRI may make available on a case-by-case basis an informal assessment of the applicable U.S. export classification for specific EPRI Intellectual Property, you and your company acknowledge that this assessment is solely for informational purposes and not for reliance purposes. You and your company acknowledge that it is still the obligation of you and your company to make your own assessment of the applicable U.S. export classification and ensure compliance accordingly. You and your company understand and acknowledge your obligations to make a prompt report to EPRI and the appropriate authorities regarding any access to or use of EPRI Intellectual Property hereunder that may be in violation of applicable U.S. or foreign export laws or regulations.

The Electric Power Research Institute Inc., (EPRI, www.epri.com) conducts research and development relating to the generation, delivery and use of electricity for the benefit of the public. An independent, nonprofit organization, EPRI brings together its scientists and engineers as well as experts from academia and industry to help address challenges in electricity, including reliability, efficiency, health, safety and the environment. EPRI also provides technology, policy and economic analyses to drive long-range research and development planning, and supports research in emerging technologies. EPRI's members represent more than 90 percent of the electricity generated and delivered in the United States, and international participation extends to 40 countries. EPRI's principal offices and laboratories are located in Palo Alto, Calif.; Charlotte, N.C.; Knoxville, Tenn.; and Lenox, Mass.

Together…Shaping the Future of Electricity

© 2011 Electric Power Research Institute (EPRI), Inc. All rights reserved. Electric Power Research Institute, EPRI, and TOGETHER…SHAPING THE FUTURE OF ELECTRICITY are registered service marks of the Electric Power Research Institute, Inc.

1021887

Electric Power Research Institute
3420 Hillview Avenue, Palo Alto, California 94304-1338 • PO Box 10412, Palo Alto, California 94303-0813 • USA
800.313.3774 • 650.855.2121 • askepri@epri.com • www.epri.com